Journal of Applied Analysis and Computation
Volume 14, Number 1, February 2024, 473–505
Website:http://www.jaac-online.com
DOI:10.11948/20230290

EFFECT OF NONLOCAL DELAY WITH STRONG KERNEL ON VEGETATION PATTERN

Juan Liang[1,2,3] and Guiquan Sun[2,4,†]

Abstract In order to understand the mechanism of water uptake by vegetation, we propose a vegetation-water model with nonlocal effect which is characterised by nonlocal delay with strong kernel in this paper. By mathematical analysis, the condition of producing steady pattern is obtained. Furthermore, the amplitude equation which determines the type of Turing pattern is obtained by nonlinear analysis method. The corresponding vegetation pattern and evolution process under different intensity of nonlocal effect in roots of vegetation are given by numerical simulations. The numerical results show that as intensity of nonlocal effect increases, the isolation degree of vegetation pattern increases which indicates that the robustness of the ecosystem decreases. Besides, the results reveal that with the water diffusion coefficient increases, the change of pattern structure is: stripe pattern→mixed pattern→spot pattern. Our results show the effects of diffusion coefficient and intensity of nonlocal effect on vegetation distribution, which provide theoretical basis for the study of vegetation.

Keywords Vegetation, pattern, nonlocal delay, multi-scale theory.

MSC(2010) 34C23, 34K20.

1. Introduction

Vegetation plays an extremely important role in ecological protection. It is beneficial to changing the abiotic environment and redistribution of resources [12]. In particular, in the process of photosynthesis, plants absorb a large amount of carbon dioxide and release oxygen, which can achieve the purpose of purifying air and improving air quality. In addition, vegetation has a strong role in soil and water conservation. The roots of the vegetation retain water to form fertile soil [43]. Therefore, the destruction of vegetation can inevitably lead to the imbalance of ecological system.

In arid or semi-arid areas, water is the decisive factor restricting the growth of vegetation. A univariate vegetation model was studied and described the dynamics

[†]The corresponding author.
[1]Data Science and Technology, North University of China, Taiyuan 030051, China
[2]Department of Mathematics, North University of China, Taiyuan 030051, China
[3]Department of Science, Taiyuan Institute of Technology, Taiyuan 030008, China
[4]Complex Systems Research Center, Shanxi University, Taiyuan 030006, China
Email: liangjuan76@126.com(J. Liang), gquansun@126.com(G. Sun)

of vegetation growth. This paper revealed that water resource was scarce in arid or semi-arid regions, there were spatial mechanisms of short distance promotion and long distance inhibition between vegetation [31]. In 1999, Klausmeier proposed the reaction-diffusion equation of two-variable vegetation and water, and the formation mechanism of stripe pattern was revealed [29]. Then, a three-dimensional model was proposed by Rietkerk et al., which was divided into vegetation, surface water and ground water [22]. So far, there has been much research on vegetation models [3, 4, 11, 27, 34, 35, 53]. Vegetation pattern is the direct reflection of vegetation spatial distribution. The spatial density distribution of vegetation and the stability of spatial structure can be seen [8,16,23–26,30,32,44,50]. Vegetation pattern can provide early warning of desertification and theoretical basis for vegetation protection [28, 41, 46, 57, 58].

In recent years, there are many researches on nonlocal interaction [1,10,13,37,48]. Nonlocal actions are generally expressed as integrals in mathematical models. The dispersal of plants can be described by nonlocal integrals and thus the dispersal of seeds over long distances can be proved. The increase of seed dispersal rate is not conducive to the formation of spot pattern structure [9]. Zaytseva et al. constructed a grass sedimension dynamic model with nonlocal term, the integral term was represented by a Mexican kernel function which could reflect the scale dependence mechanism. They deduced the conditions for the generation of pattern and the factors affecting the structure of pattern [67]. In addition, nonlocal intraspecies competition can also be coupled to the predator-prey model, and it is found that nonlocal competition can lead to the formation of spatial patterns [42].

So far, most studies on vegetation are concerned with the local effects of vegetation models. In fact, the spatial organization of vegetation is generated through a new mechanism of nonlocal promotion and local inhibition [55]. There are two processes for vegetation to absorb water. First, precipitation which is the main source of water resources permeates the soil. Second, the roots of vegetation absorb water, and then convert it into their own biomass [52]. Consequently, in arid or semi-arid areas, the roots of the vegetation absorb water in a certain area around it through a certain time, and this phenomenon is called nonlocal delay mathematically.

Nonlocal delay has been studied in many fields [7, 20, 21, 54, 65, 68]. A reaction-diffusion model for studying plankton communities was developed with nonlocal delay. In particular, this model included two delays of nutrient cycle and plankton growth response and it was proved that delay can induce space-time periodic solutions [5]. Guo et al. studied the properties of spatial inhomogeneous steady-state solutions for the reaction-diffusion systems with nonlocal delay [17,18]. Some scholars have studied the properties of traveling wave solutions for systems of partial differential equations with nonlocal time delays [19, 36, 40, 59, 61–63]. A class of systems with Lotka-Volterra competition and nonlocal delay were studied, and the properties of the solution were verified [38,39,60]. Chen et al. considered a univariate diffusive logistic model with nonlocal delay. The authors studied the stability of spatial inhomogeneous equilibrium solutions and Hopf bifurcation [6]. To sum up, there are few studies on the nonlocal processes of water absorption by roots. This paper mainly studies the vegetation-water reaction-diffusion model with nonlocal delay to reveal the growth process of vegetation.

The structure of this article is as follows. Firstly, through stability analysis we get the conditions for the generation of stationary pattern. Next, amplitude equation is obtained by multiscale analysis. Finally, the influence of intensity of nonlocal effect τ and diffusion coefficient β on the pattern structure are analyzed by numerical simulations and some important conclusions are given.

2. Model derivation and stability analysis

The two-variable mathematical model which was composed by Klausmeier in 1999 is the following form [29]:

$$\begin{cases} \dfrac{\partial N}{\partial T} = FJWN^2 - BN + D\Delta N, \\ \dfrac{\partial W}{\partial T} = R - IW - FWN^2 + \bar{V}\frac{\partial W}{\partial X}, \end{cases} \tag{2.1}$$

where N and W represent plant biomass (N) and water (W), respectively. R represents the rate of rainfall which is the supply of water and IW denotes lost rate due to evaporation. Plant absorbs water at a rate of FWN^2 and the rate of conversion to biomass is J. BN is the natural mortality of plant. $\bar{V}\frac{\partial W}{\partial X}$ is the run-off and the water flows downhill. D is the diffusion rate of plant and $\Delta = \frac{\partial^2}{\partial X^2} + \frac{\partial^2}{\partial Y^2}$.

In this paper, we mainly study the nonlocal process of water uptake by plants, a integra is introduced as follows [15, 66]:

$$\tilde{V} = \int_{\Phi}\int_{-\infty}^{t} G(x, y, t-s)f(t-s)W(y, s)dsdy,$$

where $\Phi \in [\tilde{a}, \tilde{b}] \times [\tilde{a}, \tilde{b}]$ and $x, y \in \Phi$, $G(x, y, t)f(t)$ represents the weight of the water from other positions to current position before time t. The integral is the average value of water absorption by roots of vegetation at position x.

$G(x, y, t)$ is the solution of the following equation

$$\frac{\partial G}{\partial t} = D\left(\frac{\partial^2 G}{\partial x^2} + \frac{\partial^2 G}{\partial y^2}\right)$$

and

$$\frac{\partial G}{\partial n} = 0, G(x, y, 0) = \delta(x-y).$$

Time distribution function $f(t)$ represents the water absorption strength of the roots and is selected the Gamma function ($K = 0, 1, 2, ...$):

$$f(t) = \frac{t^K e^{-\frac{t}{\tau}}}{\tau^{K+1}\Gamma(K+1)}.$$

Choose $K = 0$ and $K = 1$, and function $f(t)$ have the following forms [15]:

$$f_0(t) = \frac{1}{\tau}e^{-\frac{t}{\tau}}, f_1(t) = \frac{t}{\tau^2}e^{-\frac{t}{\tau}},$$

which represent weak kernel and strong kernel, respectively. Figure 1 shows the variations of the weak kernel and strong kernel with respect to time t, respectively. As can be seen from Figure 1(A), the weak kernel function $f_0(t)$ decreases with as time goes on, which biologically reflects that the water absorption strength of the roots decreases over time. For strong kernel $f_1(t)$, its graph increases firstly and then decreases over time, which reflects in arid or semi-arid areas vegetation is severely short of water, the strength of water absorption of the root is strong at first, then water resource near the roots of vegetation is reduced and the water absorption intensity is weakened. Obviously, strong kernel are more practical. Besides, there are few studies on nonlocal delay with strong kernel in vegetation system. Hence, this paper mainly considers the effect of strong kernel on vegetation pattern. Incor-

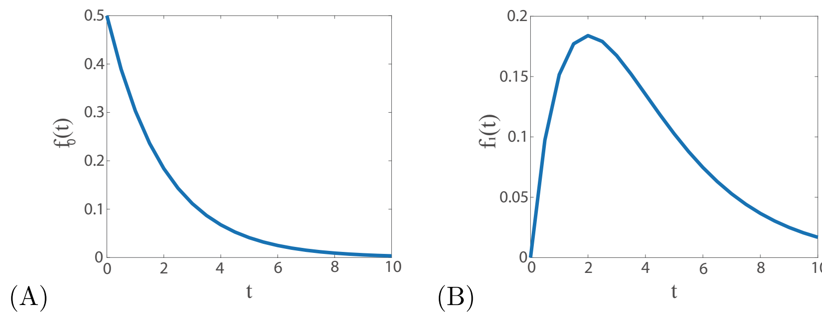

Figure 1. Image of the weak kernel (A) and strong kernel (B) over time.

porating the above mentioned nonlocal action into (2.1), the following system can be obtained:

$$\begin{cases} \dfrac{\partial N}{\partial T} = FJN^2 \int_\Phi \int_{-\infty}^{t} G(x,y,t-s) f(t-s) W(y,s) ds dy - BN + D\Delta N, \\ \dfrac{\partial W}{\partial T} = R - IW - FN^2 \int_\Phi \int_{-\infty}^{t} G(x,y,t-s) f(t-s) W(y,s) ds dy \\ \qquad + \bar{V}\frac{\partial W}{\partial X} + \bar{D}\Delta W. \end{cases} \tag{2.2}$$

Suppose the boundary condition of system (2.2) is Neuman boundary, and the initial value is nonnegative. We mainly consider the growth of vegetation on flat ground. Consequently, system (2.2) can be rewritten as follows:

$$\begin{cases} \dfrac{\partial N}{\partial T} = FJN^2 \int_\Phi \int_{-\infty}^{t} G(x,y,t-s) f(t-s) W(y,s) ds dy - BN + D\Delta N, \\ \dfrac{\partial W}{\partial T} = R - IW - FN^2 \int_\Phi \int_{-\infty}^{t} G(x,y,t-s) f(t-s) W(y,s) ds dy + \bar{D}\Delta W. \end{cases} \tag{2.3}$$

Let $\tilde{V} = \int_\Phi \int_{-\infty}^{t} G(x,y,t-s) \frac{t-s}{\tau^2} e^{-\frac{t-s}{\tau}} W(y,s) ds dy$, $f(t) = \frac{t}{\tau^2} e^{-\frac{t}{\tau}}$, system (2.3) becomes the following form [15]:

$$\begin{cases} \dfrac{\partial N}{\partial T} = FJN^2 \tilde{V} - BN + D\Delta N, \\ \dfrac{\partial W}{\partial T} = R - IW - FN^2 \tilde{V} + \bar{D}\Delta W, \\ \dfrac{\partial \tilde{V}}{\partial T} = \dfrac{1}{\tau}(P - \tilde{V}) + D\Delta \tilde{V}, \\ \dfrac{\partial P}{\partial T} = \dfrac{1}{\tau}(W - P) + D\Delta P, \end{cases} \tag{2.4}$$

where $P = \int_\Phi \int_{-\infty}^{t} G(x,y,t-s) \frac{1}{\tau} e^{-\frac{t-s}{\tau}} W(y,s) ds dy$.

Next, we prove that systems (2.3) and (2.4) are equivalent. Firstly, the following lemma is given.

Lemma 2.1. *Let Φ is a bounded domain in $\mathbb{R}^2$ and the boundary is smooth, $W(x,t) : \Phi \times (t_0, +\infty)$ is continuous and $P(x,t) \in C^{2,1}(\Phi \times [t_0, +\infty)) \bigcap C^0(\Phi \times [t_0, +\infty))$ satisfies*

$$\begin{cases} \dfrac{\partial P}{\partial T} = \dfrac{1}{\tau}(W - P) + D\Delta P, & x \in \Phi, t > t_0, \\ \dfrac{\partial P}{\partial \overrightarrow{n}} = 0, & x \in \partial\Phi, t \geq t_0, \\ P(x,t_0) = P_0(x), & x \in \Phi. \end{cases} \tag{2.5}$$

Then $P = \int_\Phi \int_{-\infty}^t G(x,y,t-s)\frac{1}{\tau}e^{-\frac{t-s}{\tau}}W(y,s)dsdy$ as $t \to +\infty$.

Proof. Suppose that $\{(\upsilon_n, \psi_n(x))\}|_{n=1}^{\infty}$ is the eigenvalues and the corresponding normalized eigenfunctions of

$$\begin{cases} -\triangle\psi(x) = \upsilon\psi(x), & x \in \Phi, \\ \dfrac{\partial \psi}{\partial \overrightarrow{n}} = 0, & x \in \partial\Phi. \end{cases}$$

The for the equation

$$\begin{cases} \mu_t(x,t) = -\dfrac{1}{\tau}\mu + D\Delta\mu, & x \in \Phi, t > t_0, \\ \dfrac{\partial \mu}{\partial \overrightarrow{n}} = 0, & x \in \partial\Phi, t \geq t_0, \\ \mu(x,t_0) = \mu_0(x), & x \in \Phi, \end{cases}$$

the solution of this equation is $\mu(x,t) = \sum\limits_{n=1}^{\infty} c_n e^{-(D\upsilon_n + \frac{1}{\tau})(t-t_0)}\psi_n(x)$, where $c_n = \int_\Phi \psi_n(y)\mu_0(y)dy$. Therefore, one has:

$$\begin{aligned} \mu(x,t) &= \int_\Phi (\sum_{n=1}^{\infty} e^{-(D\upsilon_n)(t-t_0)}\psi_n(x)\psi_n(y))e^{-\frac{1}{\tau}(t-t_0)}\mu_0(t_0)dy \\ &= \int_\Phi G(x,y,t-t_0)e^{-\frac{1}{\tau}(t-t_0)}\mu_0(y)dy. \end{aligned} \tag{2.6}$$

Similarly, let

$$\begin{cases} \overline{\mu}_t(x,t) = \dfrac{1}{\tau}W(x,t) + D\Delta\overline{\mu}, & x \in \Phi, \\ \dfrac{\partial \overline{\mu}}{\partial \overrightarrow{n}} = 0, & x \in \partial\Phi, t \geq t_0, \\ \overline{\mu}(x,t_0) = \overline{\mu}_0(x), & x \in \Phi, \end{cases}$$

a particular solution to the above equation is

$$\overline{\mu}_t(x,t) = \int_{t_0}^t \int_\Phi G(x,y,t-t_0)e^{-\frac{1}{\tau}(t-s)}W(y,s)dyds.$$

Applying the Duhamel principle, the solution of (2.5) is

$$
\begin{aligned}
P(x,t) =& \int_\Phi G(x,y,t-t_0)e^{-\frac{1}{\tau}(t-t_0)}P_(y,t_0)dy \\
&+ \int_{t_0}^{t}\int_\Phi G(x,y,t-t_0)e^{-\frac{1}{\tau}(t-s)}W(y,s)dyds.
\end{aligned}
$$

Then $\mu(x,t) \to 0$ as $t \to \infty$. Therefore, we have

$$
P = \int_\Phi \int_{-\infty}^{t} G(x,y,t-s)\frac{1}{\tau}e^{-\frac{t-s}{\tau}}W(y,s)dsdy \quad \text{as} \quad t \to +\infty.
$$

□

It is important to note that Turing pattern generation is the asymptotic behavior when $t \to \infty$. According to the Lemma 2.1 and the conclusions of references [14, 15], (2.3) and (2.4) can be regarded as equivalent. Therefore, if $(N(x,y), W(x,y), \tilde{V}(x,y), P(x,y))$ is the steady state solution of system (2.4), then $(N(x,y), W(x,y))$ is the steady state solution of (2.3).

We perform nondimensionalization:

$$
\begin{aligned}
&n = \frac{\sqrt{F}}{\sqrt{I}}N,\ w = \frac{\sqrt{F}J}{\sqrt{I}}W,\ t = IT,\ \gamma = \frac{B}{I},\ \beta = \frac{\bar{D}}{D}, \eta = \frac{\sqrt{F}J}{I\sqrt{I}}R, \\
&v = \frac{\sqrt{F}J}{\sqrt{I}}\tilde{V},\ p = \frac{\sqrt{F}J}{\sqrt{I}}P,\ \overline{x} = \frac{\sqrt{I}}{\sqrt{D}}x,\ \overline{y} = \frac{\sqrt{I}}{\sqrt{D}}y.
\end{aligned}
$$

Then the resulted nondimensionalized system is:

$$
\begin{cases}
\dfrac{\partial n}{\partial t} = n^2 v - \gamma n + \Delta n, \\
\dfrac{\partial w}{\partial t} = \eta - w - n^2 v + \beta \Delta w, \\
\dfrac{\partial v}{\partial t} = \dfrac{1}{\tau}(p - v) + \Delta v, \\
\dfrac{\partial p}{\partial t} = \dfrac{1}{\tau}(w - p) + \Delta p.
\end{cases}
\tag{2.7}
$$

By calculating that system (2.7) has three equilibria:

$$
\begin{aligned}
E_0 =& (n_0, w_0, v_0, p_0) = (0, \eta, \eta, \eta), \\
E_1 =& (n_1, w_1, v_1, p_1) \\
=& \left(\frac{2\gamma}{\eta + \sqrt{\eta^2 - 4\gamma^2}}, \frac{\eta + \sqrt{\eta^2 - 4\gamma^2}}{2}, \frac{\eta + \sqrt{\eta^2 - 4\gamma^2}}{2}, \frac{\eta + \sqrt{\eta^2 - 4\gamma^2}}{2} \right), \\
E_2 =& (n_2, w_2, v_2, p_2) \\
=& \left(\frac{2\gamma}{\eta - \sqrt{\eta^2 - 4\gamma^2}}, \frac{\eta - \sqrt{\eta^2 - 4\gamma^2}}{2}, \frac{\eta - \sqrt{\eta^2 - 4\gamma^2}}{2}, \frac{\eta - \sqrt{\eta^2 - 4\gamma^2}}{2} \right).
\end{aligned}
$$

The equilibrium E_0 is also called as the bare-soil and the two nonnegative equilibria should satisfy $\eta > 2\gamma$. Next, we mainly analyze the stability of the positive equilibria E_1 and E_2.

2.1. Stability of the equilibrium E_1

Next we linearize system (2.7) at the equilibrium E_1 when there is in the absence of diffusion, and obtain the following system:

$$\begin{cases} \dfrac{dn}{dt} = a_{11}n + a_{12}w + a_{13}v + a_{14}p, \\ \dfrac{dw}{dt} = a_{21}n + a_{22}w + a_{23}v + a_{24}p, \\ \dfrac{dv}{dt} = a_{31}n + a_{32}w + a_{33}v + a_{34}p, \\ \dfrac{dp}{dt} = a_{41}n + a_{42}w + a_{43}v + a_{44}p, \end{cases} \tag{2.8}$$

where,

$$a_{11} = \gamma,\ a_{12} = 0,\ a_{13} = \frac{\eta - \sqrt{\eta^2 - 4\gamma^2}}{\eta + \sqrt{\eta^2 - 4\gamma^2}},\ a_{14} = 0,$$

$$a_{21} = -2\gamma,\ a_{22} = -1,\ a_{23} = -\frac{\eta - \sqrt{\eta^2 - 4\gamma^2}}{\eta + \sqrt{\eta^2 - 4\gamma^2}},\ a_{24} = 0,$$

$$a_{31} = 0, a_{32} = 0,\ a_{33} = -\frac{1}{\tau},\ a_{34} = \frac{1}{\tau},$$

$$a_{41} = 0,\ a_{42} = \frac{1}{\tau},\ a_{43} = 0,\ a_{44} = -\frac{1}{\tau}.$$

The characteristic equation of system (2.8) is as follows:

$$\lambda^4 + \bar{\Upsilon}_1(0)\lambda^3 + \bar{\Upsilon}_2(0)\lambda^2 + \bar{\Upsilon}_3(0)\lambda + \bar{\Upsilon}_4(0) = 0,$$

where,

$$\bar{\Upsilon}_1(0) = 1 - \gamma + \frac{2}{\tau},\ \bar{\Upsilon}_2(0) = \frac{2}{\tau^2} + \frac{2(1-\gamma)}{\tau} - \gamma,$$

$$\bar{\Upsilon}_3(0) = \frac{a_{13} + 1 - 2\gamma}{\tau^2} - \frac{2\gamma}{\tau},\ \bar{\Upsilon}_4(0) = \frac{\gamma}{\tau^2}(a_{13} - 1).$$

According to Routh-Hurwite criterion, E_1 is stable if and only if $Re\lambda_i < 0$, then the following conditions hold:

$$\begin{cases} \bar{\Upsilon}_1(0) > 0,\ \bar{\Upsilon}_2(0) > 0,\ \bar{\Upsilon}_4(0) > 0, \\ \bar{\Upsilon}_1(0)\bar{\Upsilon}_2(0)\bar{\Upsilon}_3(0) > \bar{\Upsilon}_3^2(0) + \bar{\Upsilon}_1^2(0)\bar{\Upsilon}_4(0), \\ \bar{\Upsilon}_1(0)\bar{\Upsilon}_2(0) > \bar{\Upsilon}_3(0). \end{cases} \tag{2.9}$$

Since $a_{13} < 1$, it is easy to see that $\bar{\Upsilon}_4(0) < 0$. This is a contradiction with (2.9). Therefore, E_1 is unstable.

2.2. Stability of the equilibrium E_2

Linearzing system (2.7) near $E_2(n_2, w_2, v_2, p_2)$, we obtain the linear system as follows:

$$\begin{cases} \dfrac{\partial n}{dt} = b_{11}n + b_{12}w + b_{13}v + b_{14}p + \Delta n, \\ \dfrac{\partial w}{dt} = b_{21}n + b_{22}w + b_{23}v + b_{24}p + \beta\Delta w, \\ \dfrac{\partial v}{dt} = b_{31}n + b_{32}w + b_{33}v + b_{34}p + \Delta v, \\ \dfrac{\partial p}{dt} = b_{41}n + b_{42}w + b_{43}v + b_{44}p + \Delta p, \end{cases} \tag{2.10}$$

where,

$$\begin{aligned} &b_{11} = \gamma,\ b_{12} = 0,\ b_{13} = \frac{\eta + \sqrt{\eta^2 - 4\gamma^2}}{\eta - \sqrt{\eta^2 - 4\gamma^2}},\ b_{14} = 0, \\ &b_{21} = -2\gamma,\ b_{22} = -1,\ b_{23} = -\frac{\eta + \sqrt{\eta^2 - 4\gamma^2}}{\eta - \sqrt{\eta^2 - 4\gamma^2}},\ b_{24} = 0, \\ &b_{31} = 0,\ b_{32} = 0,\ b_{33} = -\frac{1}{\tau},\ b_{34} = \frac{1}{\tau}, \\ &b_{41} = 0,\ b_{42} = \frac{1}{\tau},\ b_{43} = 0,\ b_{44} = -\frac{1}{\tau}. \end{aligned}$$

Let

$$\begin{pmatrix} n \\ w \\ v \\ p \end{pmatrix} = \begin{pmatrix} n* \\ w* \\ v* \\ p* \end{pmatrix} + \begin{pmatrix} c_1 \\ c_2 \\ c_3 \\ c_4 \end{pmatrix} e^{\lambda t + i\vec{k}\vec{r}} + c.c + O(\varepsilon^2),$$

where $\vec{k} = (k_x, k_y)$, $\vec{r} = (X, Y)$, $c.c$ represents all complex conjugate, λ is the growth rate of perturbation in time t and $i^2 = -1$. We substitute the above equation into (2.10) to get the characteristic equation:

$$detA = \begin{vmatrix} b_{11} - \kappa^2 - \lambda & b_{12} & b_{13} & b_{14} \\ b_{21} & b_{22} - \beta k^2 - \lambda & b_{23} & b_{24} \\ b_{31} & b_{32} & b_{33} - k^2 - \lambda & b_{34} \\ b_{41} & b_{42} & b_{43} & b_{44} - \kappa^2 - \lambda \end{vmatrix} = 0,$$

which is equivalent to:

$$\lambda^4 + \bar{\Upsilon}_1(k)\lambda^3 + \bar{\Upsilon}_2(k)\lambda^2 + \bar{\Upsilon}_3(k)\lambda + \bar{\Upsilon}_4(k) = 0,$$

where,

$$\begin{aligned} &\bar{\Upsilon}_1(k) \\ =&(\beta + 3)k^2 + \frac{-\gamma\tau + \tau + 2}{\tau}, \end{aligned}$$

$$
\begin{aligned}
&\bar{\Upsilon}_2(k)\\
=&(3\beta+3)k^4-\frac{\beta\gamma\tau+2\gamma\tau-2\beta-3\tau-4}{\tau}k^2-\frac{\gamma\tau^2+2\gamma\tau-2\tau-1}{\tau^2},\\
&\bar{\Upsilon}_3(k)\\
=&(3\beta+1)k^6-\frac{2\beta\gamma\tau+\gamma\tau-4\beta-3\tau-2}{\tau}k^4-\frac{2\beta\gamma\tau+2\gamma\tau^2+2\gamma\tau-\beta-4\tau-1}{\tau^2}k^2\\
&-\frac{1}{\tau^2(\eta\rho-\eta^2+2\gamma^2)}(2\rho\eta\gamma\tau-2\eta^2\gamma\tau+4\gamma^3\tau+\rho\eta\gamma-\eta^2\gamma+2\gamma^3-\eta\rho+\eta^2),\\
&\bar{\Upsilon}_4(k)\\
=&\beta k^8-\frac{\beta\gamma\tau-2\beta-\tau}{\tau}k^6-\frac{2\beta\gamma\tau+\gamma\tau^2-\beta-2\tau}{\tau^2}k^4-\frac{1}{\tau^2(\eta\rho-\eta^2+2\gamma^2)}\\
&(\rho\eta\beta\gamma+2\rho\eta\gamma\tau-\eta^2\beta\gamma-2\eta^2\gamma\tau+2\beta\gamma^3+4\gamma^3\tau-\eta\rho+\eta^2)k^2\\
&-\frac{\gamma(\eta\rho-\eta^2+4\gamma^2)}{\tau^2(\eta\rho-\eta^2+2\gamma^2)},
\end{aligned}
$$

where $\rho=\sqrt{(\eta+2\gamma)(\eta-2\gamma)}$.

The characteristic equation of the system (2.7) without the diffusion term is:

$$\mu^4+\bar{\Upsilon}_1(0)\mu^3+\bar{\Upsilon}_2(0)\mu^2+\bar{\Upsilon}_3(0)\mu+\bar{\Upsilon}_4(0)=0,$$

where,

$$
\begin{aligned}
\bar{\Upsilon}_1(0)&=\frac{-\gamma\tau+\tau+2}{\tau},\ \bar{\Upsilon}_2(0)=-\frac{\gamma\tau^2+2\gamma\tau-2\tau-1}{\tau^2},\\
\bar{\Upsilon}_3(0)&=-\frac{1}{\tau^2(\eta\rho-\eta^2+2\gamma^2)}(2\rho\eta\gamma\tau-2\eta^2\gamma\tau+4\gamma^3\tau\\
&\quad+\rho\eta\gamma-\eta^2\gamma+2\gamma^3-\eta\rho+\eta^2),\\
\bar{\Upsilon}_4(0)&=-\frac{\gamma(\gamma\rho-\eta^2+4\gamma^2)}{\tau^2(\eta\rho-\eta^2+2\gamma^2)}.
\end{aligned}
$$

We have that E_2 is stable if and only if (2.9) holds. In the case when there is diffusion in system (2.7), the conditions for stability of the equilibrium are as follows:

$$
\begin{cases}
(1)\bar{\Upsilon}_1(k)>0,\ \bar{\Upsilon}_2(k)>0,\ \bar{\Upsilon}_4(k)>0,\\
(2)\bar{\Upsilon}_1(k)\bar{\Upsilon}_2(k)\bar{\Upsilon}_3(k)>\bar{\Upsilon}_3^2(k)+\bar{\Upsilon}_1^2(k)\bar{\Upsilon}_4(k),\\
(3)\bar{\Upsilon}_1(k)\bar{\Upsilon}_2(k)>\bar{\Upsilon}_3(k).
\end{cases}
\tag{2.11}
$$

The steady state E_2 of the model (2.7) without diffusion is stable and if it is unstable in presence of diffusion, then Turing instability occurs [45]. Hence, the characteristic equation must have at least one positive eigenvalue or complex eigenvalues with positive real part. When (2.9) is established and one of (1)-(3) of (2.11) is not satisfied, the equilibrium becomes unstable and the Turing pattern is induced. Next, we will consider two cases in which patterns are induced.

Case 1. (a) $\bar{\Upsilon}_1(k)=(\beta+3)k^2+\dfrac{-\gamma\tau+\tau+2}{\tau}$.

Since all the parameters are nonnegative, $\bar{\Upsilon}_1(k)>0$ is always established under the condition $\bar{\Upsilon}_1(0)>0$.

(b) Let $\bar{\Upsilon}_2(k) = f_{22}z^2 + f_{21}z + f_{20}$, $z = k^2$,
where,

$$
\begin{aligned}
f_{22} &= 3\beta + 3,\\
f_{21} &= -\frac{\beta\gamma\tau + 2\gamma\tau - 2\beta - 3\tau - 4}{\tau},\\
f_{20} &= -\frac{\gamma\tau^2 + 2\gamma\tau - 2\tau - 1}{\tau^2}.
\end{aligned}
$$

Since $f_{22} > 0$, then $\bar{\Upsilon}_2(k)$ takes the minimum value when $z = -\frac{f_{21}}{2f_{22}}$,

$$\bar{\Upsilon}_2(k)_{min} = \frac{4f_{22}f_{20} - f_{21}^2}{4f_{22}}.$$

In summary, Turing patterns are induced by combining (2.9) and the following conditions:

$$
\begin{cases}
4f_{22}f_{20} - f_{21}^2 < 0,\\
f_{21} < 0.
\end{cases}
$$

(c) Let $\bar{\Upsilon}_4(k) = R(k^2) = f_{44}z^4 + f_{43}z^3 + f_{42}z^2 + f_{41}z + f_{40}$ and $z = k^2$, where,

$$
\begin{aligned}
f_{44} &= \beta,\\
f_{43} &= -\frac{\beta\gamma\tau - 2\beta - \tau}{\tau},\\
f_{42} &= -\frac{2\beta\gamma\tau + \gamma\tau^2 - \beta - 2\tau}{\tau^2},\\
f_{41} &= -\frac{1}{\tau^2(\eta\rho - \eta^2 + 2\gamma^2)}(\rho\eta\beta m + 2\rho\eta\gamma\tau - \eta^2\beta\gamma - 2\eta^2\gamma\tau\\
&\quad + 2\beta\gamma^3 + 4\gamma^3\tau - \eta\rho + \eta^2)),\\
f_{40} &= -\frac{\gamma(\eta\rho - \eta^2 + 4\gamma^2)}{\tau^2(\eta\rho - \eta^2 + 2\gamma^2)}.
\end{aligned}
$$

It is noted that $f_{44} > 0$ and $f_{40} > 0$. The first derivative of $R(z)$ is:

$$\frac{dR(z)}{dz} = 4f_{44}z^3 + 3f_{43}z^2 + 2f_{42}z + f_{41}.$$

Let $e = 4f_{44}, f = 3f_{43}, g = 2f_{42}$ and $h = f_{41}$, then we have:

$$\frac{dR(z)}{dz} = ez^3 + fz^2 + gz + h.$$

Suppose that

$$
\begin{aligned}
\varphi &= f^2 - 3eg,\\
\chi &= fg - 9eh,\\
\psi &= g^2 - 3fh,\\
\Delta &= \chi^2 - 4\varphi\psi,
\end{aligned}
$$

we can obtain some properties about polynomials $R(z)$:

For any $z = k^2$, $f_{40} > 0$ and $R(z) \to +\infty$ as $z \to +\infty$. Besides, according to Shengjin's criterion [21], we have:

When $\varphi = \chi = 0$, $\frac{dR(z)}{dz} = 0$ has three equal real roots:

$$z_1 = z_2 = z_3 = -\frac{f}{3e} = -\frac{g}{f} = -\frac{3h}{g}.$$

When $\Delta = 0$, $\frac{dR(z)}{dz} = 0$ has the roots:

$$z_1 = -\frac{f}{e} + K,\ z_2 = z_3 = -\frac{K}{2},$$

where $K = \frac{\chi}{\psi}(\psi \neq 0)$.

When $\Delta > 0$, $\frac{dR(z)}{dz} = 0$ has the following roots:

$$\begin{aligned} z_1 &= -\frac{f + \sqrt[3]{y_1} + \sqrt[3]{y_2}}{3e}, \\ z_{2,3} &= \frac{-f + \frac{1}{2}(\sqrt[3]{y_1} + \sqrt[3]{y_2}) \pm \frac{\sqrt{3}}{2}(\sqrt[3]{y_1} - \sqrt[3]{y_2})i}{3e}, \end{aligned}$$

where $y_{1,2} = \varphi f + 3e(\frac{-\chi \pm \sqrt{\chi^2 - 4\varphi\psi}}{2})$.

When $\Delta < 0$, $\frac{dR(z)}{dz} = 0$ has the roots as follows:

$$\begin{aligned} z_1 &= -\frac{f + 2\sqrt{\varphi}\cos(\frac{\phi}{3})}{3e}, \\ z_{2,3} &= \frac{-f + \sqrt{\varphi}(\cos\frac{\phi}{3} \pm \sqrt{3}\sin\frac{\phi}{3})}{3e}, \end{aligned}$$

where $\phi = \arccos T, T = \frac{2\varphi f - 3e\chi}{2\varphi\sqrt{\varphi}}(\varphi > 0, -1 < T < 1)$.

When $\bar{\Upsilon}_4(k) < 0$ and (2.9) hold, Turing pattern occurs. As a consequence, we have the following conclusion:

(1) If $\varphi = \chi = 0$, $R(z)$ has an extreme point $z_1 = -\frac{f}{3e} = -\frac{g}{f} = -\frac{3h}{g}$ and it is a minimum point and z_2 is the maximum point. The sufficient conditions for the occurrence of Turing pattern are as follows:

$$\begin{cases} z_1 > 0, \\ R(z_1) < 0. \end{cases}$$

(2) If $\Delta = 0$, $R(z)$ has two extreme points z_1, z_2 and the minimum is to the right of the maximum. The sufficient conditions for the occurrence of Turing pattern are as follows:

$$\begin{cases} \max(z_1, z_2) > 0, \\ R(\max(z_1, z_2)) < 0. \end{cases}$$

(3) If $\Delta > 0$, $R(z)$ has a real extreme point z_1. The following inequalities are the conditions for producing Turing pattern:

$$\begin{cases} z_1 > 0, \\ R(z_1) < 0. \end{cases}$$

(4) If $\Delta < 0$, $R(z)$ has three extreme points z_1, z_2, z_3. Suppose $z_1 < z_2 < z_3$, then z_1 and z_3 are the minimum points. We consider the conditions for the occurrence of Turing pattern in two cases:

When $z_1 > 0$,

$$\min\{R(z_1), R(z_3)\} < 0.$$

When $z_1 < 0$,

$$\begin{cases} z_3 > 0, \\ R(z_3) < 0. \end{cases}$$

Case 2. $\bar{\Upsilon}_1(k)\bar{\Upsilon}_2(k) < \bar{\Upsilon}_3(k)$.

Let $R_1(k^2) = \bar{\Upsilon}_1(k)\bar{\Upsilon}_2(k) - \bar{\Upsilon}_3(k)$ and $z = k^2$, then

$$R_1(z) = r_{13}z^3 + r_{12}z^2 + r_{11}z + r_{10},$$

where,

$$\begin{aligned}
r_{13} &= 3\beta^2 + 9\beta + 8, \\
r_{12} &= -\frac{1}{\tau}(\beta^2\gamma\tau + 10\beta\gamma\tau - 2\beta^2 - 6\beta\tau + 10\gamma\tau - 20\beta - 15\tau - 20), \\
r_{11} &= \frac{1}{\tau^2}(\beta\gamma^2\tau^2 - 2\beta\gamma\tau^2 + 2\gamma^2\tau^2 - 8\beta\gamma\tau - 10\gamma\tau^2 + 4\beta\tau - 16\gamma\tau + 3\tau^2 \\
&\quad + 6\beta + 20\tau + 12), \\
r_{10} &= \frac{1}{\tau^3(\eta\rho - \eta^2 + 2\gamma^2)}(\rho\eta\gamma^2\tau^3 - \eta^2\gamma^2\tau^3 + 2\gamma^4\tau^3 + 2\rho\eta\gamma^2\tau^2 - \rho\eta\gamma\tau^3 - 2\eta^2\gamma^2\tau^2 \\
&\quad + \eta^2\gamma\tau^3 + 4\gamma^2\tau^2 - 2\gamma^3\tau^3 - 8\rho\eta\gamma\tau^2 + 8\eta^2\gamma\tau^2 - 16\gamma^3\tau^2 - 6\rho\eta\gamma\tau + 2\rho\eta\tau^2 \\
&\quad + 6\eta^2\gamma\tau - 2\eta^2\tau^2 - 12\gamma^3\tau + 6\rho\eta\tau - 6\eta^2\tau + 10\gamma^2\tau + 2\eta\rho - 2\eta^2 + 4\gamma^2).
\end{aligned}$$

It is easy to verify that for any $z = k^2$, $R_1(z) \to +\infty$ when $z \to +\infty$. Furthermore, the first derivative of $R_1(z)$ is:

$$\frac{dR_1(z)}{dz} = 3r_{13}z^2 + 2r_{12}z + r_{11} = 0.$$

The equation has two roots, which implies $R_1(z)$ has two extreme points:

$$z_1 = \frac{-r_{12} + \sqrt{r_{12}^2 - 3r_{13}r_{11}}}{3r_{13}}$$

and

$$z_2 = \frac{-r_{12} - \sqrt{r_{12}^2 - 3r_{13}r_{11}}}{3r_{13}}.$$

Applying the above analysis, it yields

$$z_{\max} = z_2 < z_{\min} = z_1.$$

When $R_1(z)_{\min} = R_1(z_1) < 0$, the pattern is induced. The minimum point z_1 is the square of the wave number k, and it should be guaranteed to be positive.

Based the above analysis, the system (2.7) produces Turing bifurcation when the conditions are certified:

$$\begin{cases} r_{12}^2 - 3r_{13}r_{11} > 0, \\ z_1 > 0, \\ R_1(z_1) < 0. \end{cases}$$

Case 3. $\bar{\Upsilon}_1(k)\bar{\Upsilon}_2(k)\bar{\Upsilon}_3(k) > \bar{\Upsilon}_3^2(k) + \bar{\Upsilon}_1^2(k)\bar{\Upsilon}_4(k)$.

This case is complicated to analyze and we do not consider it in this paper.

We show the dispersion relation in Fig. 2 with fixed parameters: $\eta = 2.6, \gamma = 1.2, \beta = 30$, and τ has different values. Turing patterns are induced under the conditions $\mathrm{Re}(\lambda) < 0$ when $k = 0$ and $\mathrm{Re}(\lambda) > 0$ when $k > 0$.

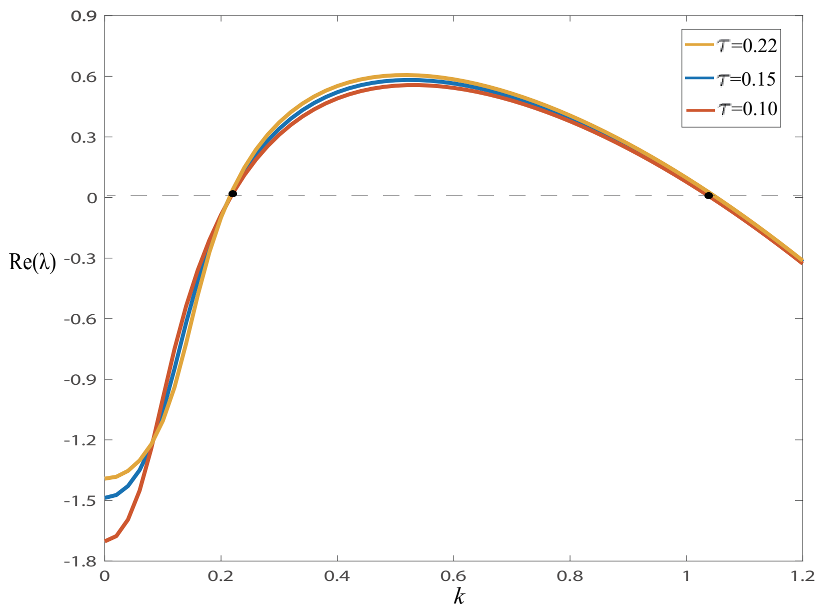

Figure 2. Dispersion relation of system (2.7). In the case of fixed other parameters: $\eta = 2.6, \gamma = 1.2, \beta = 30$, τ takes four different values. When τ takes different values, with the increase of k, the real part of the characteristic root is greater than zero, the spatial pattern of system (2.7) is generated. The black dots is the critical points of $Re(\lambda) < 0$.

3. Multiple scale analysis

In this part, we derive the amplitude equation to reveal the spatiotemporal behavior of the attachment of Turing bifurcation points [21,52]. Only when the wave number disturbance approaches the critical value k_T, the steady state solution will become unstable. This paper mainly studies the vegetation-water model, and the process of changing pattern structure by controlling the parameters of amplitude equation is studied. In order to obtain the control parameter τ, the critical wave number $k = k_T$ is calculated at first. Substituting k_T into $\Upsilon_4(k) = 0$, bifurcation threshold τ_T is obtained.

We rewrite the system (2.7) at the equilibrium $E_2 = (N_2, W_2, V_2, P_2)$:

$$\begin{cases} \dfrac{\partial n}{\partial t} = b_{11}n + b_{12}w + b_{13}v + b_{14}p + N_1(n, w, v, p) + \Delta n, \\ \dfrac{\partial w}{\partial t} = b_{21}n + b_{22}w + b_{23}v + b_{24}p + N_2(n, w, v, p) + \beta\Delta w, \\ \dfrac{\partial v}{\partial t} = b_{31}n + b_{32}w + b_{33}v + b_{34}p + N_3(n, w, v, p) + \Delta v, \\ \dfrac{\partial p}{\partial t} = b_{41}n + b_{42}w + b_{43}v + b_{44}p + N_4(n, w, v, p) + \Delta p, \end{cases} \tag{3.1}$$

where,

$$N_1(n, w, v, p) = n^2 w,$$

$$N_2(n, w, v, p) = -n^2 w,$$

$$N_3(n, w, v, p) = 0,$$

$$N_4(n, w, v, p) = 0.$$

Since near the onset $\tau = \tau_T$, the following expression is a form of the solution of system (2.7):

$$U = U_u + \sum_{j=1}^{3} U_0[A_j e^{i\vec{k_j}\cdot\vec{r}} + \vec{A}_j e^{-i\vec{k_j}\cdot\vec{r}}],$$

where $\vec{k_j}$ and $-\vec{k_j}$ are a pair of oscilatory wave vectors and $|k_j| = k_T$, and the direction is different.

Take advantage of the above formula, we can obtain the solution of (2.7) as the following form:

$$U^0 = \sum_{j=1}^{3} U_0[A_j e^{i\vec{k_j}\cdot\vec{r}} + \bar{A}_j e^{-i\vec{k_j}\cdot\vec{r}}].$$

Let $U = (n, w, v, p)^T$ and $N = (N_1, N_2, N_3, N_4)^T$, then system (2.7) can be rewritten as:

$$\frac{\partial U}{\partial t} = LU + N, \tag{3.2}$$

where,

$$L = \begin{pmatrix} b_{11} + \Delta & b_{12} & b_{13} & b_{14} \\ b_{21} & b_{22} + \delta\Delta & b_{23} & b_{24} \\ b_{31} & b_{32} & b_{33} + \Delta & b_{34} \\ b_{41} & b_{42} & b_{43} & b_{44} + \Delta \end{pmatrix}.$$

Let

$$L = L_T + (\tau_T - \tau)M, \tag{3.3}$$

where,

$$L_T = \begin{pmatrix} a_{11}^* + \Delta & a_{12}^* & a_{13}^* & a_{14}^* \\ a_{21}^* & a_{22}^* + \delta\Delta & a_{23}^* & a_{24}^* \\ a_{31}^* & a_{32}^* & a_{33}^* + \Delta & a_{34}^* \\ a_{41}^* & a_{42}^* & a_{43}^* & a_{44}^* + \Delta \end{pmatrix},$$

and

$$M = \begin{pmatrix} m_{11} & m_{12} & m_{13} & m_{14} \\ m_{21} & m_{22} & m_{23} & m_{24} \\ m_{31} & m_{32} & m_{33} & m_{34} \\ m_{41} & m_{42} & m_{43} & m_{44} \end{pmatrix},$$

$$\begin{aligned}
&a_{11}^* = b_{11},\ a_{12}^* = 0,\ a_{13}^* = b_{13},\ a_{14}^* = 0,\\
&a_{21}^* = b_{21},\ a_{22}^* = b_{22},\ a_{23}^* = b_{23},\ a_{24}^* = 0,\\
&a_{31}^* = 0,\ a_{32}^* = 0,\ a_{33}^* = -\tfrac{1}{\tau},\ a_{34}^* = \tfrac{1}{\tau},\\
&a_{41}^* = 0,\ a_{42}^* = \tfrac{1}{\tau},\ a_{43}^* = 0,\ a_{44}^* = -\tfrac{1}{\tau},\\
&m_{11} = \tfrac{b_{11}-a_{11}^*}{\tau_T-\tau},\ m_{12} = \tfrac{b_{12}-a_{12}^*}{\tau_T-\tau},\ m_{13} = \tfrac{b_{13}-a_{13}^*}{\tau_T-\tau},\ m_{14} = \tfrac{b_{14}-a_{14}^*}{\tau_T-\tau},\\
&m_{21} = \tfrac{b_{21}-a_{21}^*}{\tau_T-\tau},\ m_{22} = \tfrac{b_{22}-a_{22}^*}{\tau_T-\tau},\ m_{23} = \tfrac{b_{23}-a_{23}^*}{\tau_T-\tau},\ m_{24} = \tfrac{b_{24}-a_{24}^*}{\tau_T-\tau},\\
&m_{31} = \tfrac{b_{31}-a_{31}^*}{\tau_T-\tau},\ m_{32} = \tfrac{b_{32}-a_{32}^*}{\tau_T-\tau},\ m_{33} = \tfrac{b_{33}-a_{33}^*}{\tau_T-\tau},\ m_{34} = \tfrac{b_{34}-a_{34}^*}{\tau_T-\tau},\\
&m_{41} = \tfrac{b_{41}-a_{41}^*}{\tau_T-\tau},\ m_{42} = \tfrac{b_{42}-a_{42}^*}{\tau_T-\tau},\ m_{43} = \tfrac{b_{43}-a_{43}^*}{\tau_T-\tau},\ m_{44} = \tfrac{b_{44}-a_{44}^*}{\tau_T-\tau}.
\end{aligned}$$

Next we will use multiscale analysis, let

$$\tau_T - \tau = \varepsilon\tau_1 + \varepsilon^2\tau_2 + \varepsilon^3\tau_3 + o(\varepsilon^4), \tag{3.4}$$

$$U = \begin{pmatrix} n \\ w \\ v \\ p \end{pmatrix} = \varepsilon \begin{pmatrix} n_1 \\ w_1 \\ v_1 \\ p_1 \end{pmatrix} + \varepsilon^2 \begin{pmatrix} n_2 \\ w_2 \\ v_2 \\ p_2 \end{pmatrix} + \varepsilon^3 \begin{pmatrix} n_3 \\ w_3 \\ v_3 \\ p_3 \end{pmatrix} + o(\varepsilon^4), \tag{3.5}$$

$$N = \varepsilon^2 h_2 + \varepsilon^3 h_3 + o(\varepsilon^4), \tag{3.6}$$

where,

$$h_2 = \begin{pmatrix} h_{21} \\ h_{22} \\ 0 \\ 0 \end{pmatrix},\ h_3 = \begin{pmatrix} n_1^2 w_1 \\ -n_1^2 w_1 \\ 0 \\ 0 \end{pmatrix},$$

$$h_{21} = \frac{\eta - \sqrt{\eta^2 - 4\gamma^2}}{2} n_1^2 + \frac{\gamma}{\eta - \sqrt{\eta^2 - 4\gamma^2}} n_1 w_1,$$

$$h_{22} = -\frac{\eta - \sqrt{\eta^2 - 4\gamma^2}}{2} n_1^2 - \frac{\gamma}{\eta - \sqrt{\eta^2 - 4\gamma^2}} n_1 w_1.$$

Let

$$\frac{\partial}{\partial t} = \frac{\partial}{\partial T_0} + \varepsilon \frac{\partial}{\partial T_1} + \varepsilon^2 \frac{\partial}{\partial T_2} + o(\varepsilon^3). \tag{3.7}$$

$\frac{\partial}{\partial T_0}$ corresponds to the fast variable. Then we can obtain the following derivative:

$$\frac{\partial A}{\partial t} = \varepsilon \frac{\partial A}{\partial T_1} + \varepsilon^2 \frac{\partial A}{\partial T_2} + o(\varepsilon^3), \tag{3.8}$$

where $T_0 = t, T_1 = \varepsilon t, T_2 = \varepsilon^2 t$.

Noting (3.2) and (3.3), it can be verified the following equation:

$$\frac{\partial U}{\partial t} = (L_T + (\tau_T - \tau)M)U + N = L_T U + (\tau_T - \tau)MU + N. \tag{3.9}$$

We substitute (3.4)-(3.7) into (3.9) and obtain the following equations:

$$L_T \begin{pmatrix} n_1 \\ w_1 \\ v_1 \\ p_1 \end{pmatrix} = 0, \tag{3.10}$$

$$L_T \begin{pmatrix} n_2 \\ w_2 \\ v_2 \\ p_2 \end{pmatrix} = \frac{\partial}{\partial T_1} \begin{pmatrix} n_1 \\ w_1 \\ v_1 \\ p_1 \end{pmatrix} - \tau_1 M \begin{pmatrix} n_1 \\ w_1 \\ v_1 \\ p_1 \end{pmatrix} - h_2, \tag{3.11}$$

$$L_T \begin{pmatrix} n_3 \\ w_3 \\ v_3 \\ p_3 \end{pmatrix} = \frac{\partial}{\partial T_1} \begin{pmatrix} n_2 \\ w_2 \\ v_2 \\ p_2 \end{pmatrix} + \frac{\partial}{\partial T_2} \begin{pmatrix} n_1 \\ w_1 \\ v_1 \\ p_1 \end{pmatrix} - \tau_1 M \begin{pmatrix} n_2 \\ w_2 \\ v_2 \\ p_2 \end{pmatrix} - \tau_2 M \begin{pmatrix} n_1 \\ w_1 \\ v_1 \\ p_1 \end{pmatrix} - h_3. \tag{3.12}$$

Clearly, L_T is a linear operator at a critical point. $(n_1, w_1, v_1, p_1)^T$ is a linear combination of eigenvectors which is corresponding to eigenvalue of zero. It then follows from (3.10) that:

$$\begin{pmatrix} n_1 \\ w_1 \\ v_1 \\ p_1 \end{pmatrix} = \begin{pmatrix} l_1 \\ l_2 \\ l_3 \\ 1 \end{pmatrix} (\Theta_1 e^{i\vec{k_1}\cdot\vec{r}} + \Theta_2 e^{i\vec{k_2}\cdot\vec{r}} + \Theta_3 e^{i\vec{k_3}\cdot\vec{r}}) + c.c., \tag{3.13}$$

where,

$$l_1 = \frac{a_{13}^*}{(k_T^2 - a_{11}^*)(1+\tau k_T^2)},\ l_2 = 1+\tau k_T^2,\ l_3 = \frac{1}{1+\tau k_T^2},$$

and $K_j = K_T, j = 1,2,3$. Θ_j is the amplitude of $e^{i\vec{k_j}\cdot\vec{r}}$ under the first order perturbation.

The following expression can be deduced by Eq. (3.11) directly:

$$\begin{aligned}
&L_T \begin{pmatrix} n_2 \\ w_2 \\ v_2 \\ p_2 \end{pmatrix} \\
=&\frac{\partial}{\partial T_1}\begin{pmatrix} n_1 \\ w_1 \\ v_1 \\ p_1 \end{pmatrix} - \tau_1 M \begin{pmatrix} n_1 \\ w_1 \\ v_1 \\ p_1 \end{pmatrix} - h_2 \\
=&\frac{\partial}{\partial T_1}\begin{pmatrix} n_1 \\ w_1 \\ v_1 \\ p_1 \end{pmatrix} - \tau_1 \begin{pmatrix} m_{11}n_1 + m_{12}w_1 + m_{13}v_1 + m_{14}p_1 \\ m_{21}n_1 + m_{22}w_1 + m_{23}v_1 + m_{24}p_1 \\ m_{31}n_1 + m_{32}w_1 + m_{33}v_1 + m_{34}p_1 \\ m_{41}n_1 + m_{42}w_1 + m_{43}v_1 + m_{44}p_1 \end{pmatrix} - \begin{pmatrix} h_{21} \\ h_{22} \\ 0 \\ 0 \end{pmatrix} \\
=&\begin{pmatrix} F_n \\ F_w \\ F_v \\ F_p \end{pmatrix}.
\end{aligned} \tag{3.14}$$

Applying the Fredholm solvability condition, we conclude that a sufficient condition for (3.14) to have a nontrivial solution is that the function of the right of (3.14) is orthogonal to zero eigenvector of L_T^+ and the expression is as follows:

$$\begin{pmatrix} 1 \\ l_2^+ \\ l_3^+ \\ l_4^+ \end{pmatrix} e^{-i\vec{k_j}\cdot\vec{r}},\ j = 1,2,3,$$

where,

$$l_2^+ = \frac{d_1 k_T^2 - a_{11}^*}{a_{21}^*},$$

$$l_3^+ = \frac{\tau_T(d_1k_T^2 - a_{11}^*)(d_2k_T^2 - a_{22}^*) - \tau_T a_{12}^* a_{21}^*}{a_{21}^*},$$

$$l_4^+ = \frac{a_{11}^*}{a_{21}^*} l_2^+ l_3^+.$$

According to the orthogonal condition, we can obtain that

$$\left(1,\, l_2^+,\, l_3^+,\, l_4^+\right)\begin{pmatrix} F_n^j \\ F_w^j \\ F_v^j \\ F_p^j \end{pmatrix} = 0,$$

where $F_n^j, F_w^j, F_v^j, F_p^j$ represent the coefficients corresponding to $e^{i\vec{k_j}\cdot\vec{r}}$ in F_n, F_w, F_v, F_p, then we have:

$$\begin{pmatrix} F_n \\ F_w \\ F_v \\ F_p \end{pmatrix} = \begin{pmatrix} F_n \\ F_w \\ F_v \\ F_p \end{pmatrix} e^{i\vec{k_1}\cdot\vec{r}} + \begin{pmatrix} F_n \\ F_w \\ F_v \\ F_p \end{pmatrix} e^{i\vec{k_2}\cdot\vec{r}} + \begin{pmatrix} F_n \\ F_w \\ F_v \\ F_p \end{pmatrix} e^{i\vec{k_3}\cdot\vec{r}}.$$

Combining (3.13) with (3.14), one has:

$$\begin{pmatrix} F_n^1 \\ F_w^1 \\ F_v^1 \\ F_p^1 \end{pmatrix} = \begin{pmatrix} l_1\frac{\partial\Theta_1}{\partial T_1} \\ l_2\frac{\partial\Theta_1}{\partial T_1} \\ l_3\frac{\partial\Theta_1}{\partial T_1} \\ \frac{\partial\Theta_1}{\partial T_1} \end{pmatrix} - \tau_1 \begin{pmatrix} m_{11}l_1 + m_{12}l_2 + m_{13}l_3 + m_{14} \\ m_{21}l_1 + m_{22}l_2 + m_{23}l_3 + m_{24} \\ m_{31}l_1 + m_{32}l_2 + m_{33}l_3 + m_{34} \\ m_{41}l_1 + m_{42}l_2 + m_{43}l_3 + m_{44} \end{pmatrix} \Theta_1 + \begin{pmatrix} h_{21} \\ h_{22} \\ 0 \\ 0 \end{pmatrix} \overline{\Theta}_2\overline{\Theta}_3, \tag{3.15}$$

$$\begin{pmatrix} F_n^2 \\ F_w^2 \\ F_v^2 \\ F_p^2 \end{pmatrix} = \begin{pmatrix} l_1\frac{\partial\Theta_2}{\partial T_1} \\ l_2\frac{\partial\Theta_2}{\partial T_1} \\ l_3\frac{\partial\Theta_2}{\partial T_1} \\ \frac{\partial\Theta_2}{\partial T_1} \end{pmatrix} - \tau_1 \begin{pmatrix} m_{11}l_1 + m_{12}l_2 + m_{13}l_3 + m_{14} \\ m_{21}l_1 + m_{22}l_2 + m_{23}l_3 + m_{24} \\ m_{31}l_1 + m_{32}l_2 + m_{33}l_3 + m_{34} \\ m_{41}l_1 + m_{42}l_2 + m_{43}l_3 + m_{44} \end{pmatrix} \Theta_2 + \begin{pmatrix} h_{21} \\ h_{22} \\ 0 \\ 0 \end{pmatrix} \overline{\Theta}_1\overline{\Theta}_3, \tag{3.16}$$

$$\begin{pmatrix} F_n^3 \\ F_w^3 \\ F_v^3 \\ F_p^3 \end{pmatrix} = \begin{pmatrix} l_1\frac{\partial\Theta_3}{\partial T_1} \\ l_2\frac{\partial\Theta_3}{\partial T_1} \\ l_3\frac{\partial\Theta_3}{\partial T_1} \\ \frac{\partial\Theta_3}{\partial T_1} \end{pmatrix} - \tau_1 \begin{pmatrix} m_{11}l_1 + m_{12}l_2 + m_{13}l_3 + m_{14} \\ m_{21}l_1 + m_{22}l_2 + m_{23}l_3 + m_{24} \\ m_{31}l_1 + m_{32}l_2 + m_{33}l_3 + m_{34} \\ m_{41}l_1 + m_{42}l_2 + m_{43}l_3 + m_{44} \end{pmatrix} \Theta_3 + \begin{pmatrix} h_{21} \\ h_{22} \\ 0 \\ 0 \end{pmatrix} \overline{\Theta}_1\overline{\Theta}_2. \tag{3.17}$$

Applying the Fredholm solvability condition, we get that:

$$\begin{cases} (l_1+l_2l_2^++l_3l_3^++l_4^+)\dfrac{\partial\Theta_1}{\partial T_1} =\tau_1[(m_{11}l_1+m_{12}l_2+m_{13}l_3+m_{14})+l_2^+(m_{21}l_1 \\ \qquad +m_{22}l_2+m_{23}l_3+m_{24})+l_3^+(m_{31}l_1+m_{32}l_2 \\ \qquad +m_{33}l_3+m_{34})+(m_{41}l_1+m_{42}l_2+m_{43}l_3 \\ \qquad +m_{44})]\Theta_1-(h_{21}+l_2^+h_{22})\overline{\Theta}_2\overline{\Theta}_3, \\ (l_1+l_2l_2^++l_3l_3^++l_4^+)\dfrac{\partial\Theta_2}{\partial T_1} =\tau_1[(m_{11}l_1+m_{12}l_2+m_{13}l_3+m_{14})+l_2^+(m_{21}l_1 \\ \qquad +m_{22}l_2+m_{23}l_3+m_{24})+l_3^+(m_{31}l_1+m_{32}l_2 \\ \qquad +m_{33}l_3+m_{34})+(m_{41}l_1+m_{42}l_2+m_{43}l_3 \\ \qquad +m_{44})]\Theta_2-(h_{21}+l_2^+h_{22})\overline{\Theta}_1\overline{\Theta}_3, \\ (l_1+l_2l_2^++l_3l_3^++l_4^+)\dfrac{\partial\Theta_3}{\partial T_1} =\tau_1[(m_{11}l_1+m_{12}l_2+m_{13}l_3+m_{14})+l_2^+(m_{21}l_1 \\ \qquad +m_{22}l_2+m_{23}l_3+m_{24})+l_3^+(m_{31}l_1+m_{32}l_2 \\ \qquad +m_{33}l_3+m_{34})+(m_{41}l_1+m_{42}l_2+m_{43}l_3 \\ \qquad +m_{44})]\Theta_3-(h_{21}+l_2^+h_{22})\overline{\Theta}_1\overline{\Theta}_2. \end{cases} \tag{3.18}$$

The second formula of equation (3.11) is solved as follows:

$$\begin{pmatrix} n_2 \\ w_2 \\ v_2 \\ p_2 \end{pmatrix} = \begin{pmatrix} N_0 \\ W_0 \\ V_0 \\ P_0 \end{pmatrix} + \sum_{i=1}^{3} \begin{pmatrix} N_i \\ W_i \\ V_i \\ P_i \end{pmatrix} e^{i\vec{k_i}\cdot\vec{r}} + \sum_{i=1}^{3} \begin{pmatrix} N_{ii} \\ W_{ii} \\ V_{ii} \\ P_{ii} \end{pmatrix} e^{i2\vec{k_i}\cdot\vec{r}} + \begin{pmatrix} N_{12} \\ W_{12} \\ V_{12} \\ P_{12} \end{pmatrix} e^{i(\vec{k_1}-\vec{k_2})\cdot\vec{r}}$$
$$+ \begin{pmatrix} N_{23} \\ W_{23} \\ V_{23} \\ P_{23} \end{pmatrix} e^{i(\vec{k_2}-\vec{k_3})\cdot\vec{r}} + \begin{pmatrix} N_{31} \\ W_{31} \\ V_{31} \\ P_{31} \end{pmatrix} e^{i(\vec{k_3}-\vec{k_1})\cdot\vec{r}} + c.c., \tag{3.19}$$

where,

$$\begin{aligned} N_0 &= n_0(|\Theta_1|^2+|\Theta_2|^2+|\Theta_3|^2), \\ W_0 &= w_0(|\Theta_1|^2+|\Theta_2|^2+|\Theta_3|^2), \\ V_0 &= v_0(|\Theta_1|^2+|\Theta_2|^2+|\Theta_3|^2), \\ P_0 &= p_0(|\Theta_1|^2+|\Theta_2|^2+|\Theta_3|^2), \\ N_i &= l_1P_i, \end{aligned}$$

$$
\begin{aligned}
W_i &= l_2 P_i,\\
V_i &= l_3 P_i,\\
N_{ii} &= n_{11}\Theta_i^2,\\
W_{ii} &= w_{11}\Theta_i^2,\\
V_{ii} &= v_{11}\Theta_i^2,\\
P_{ii} &= p_{11}\Theta_i^2,\\
\begin{pmatrix} N_{ij}\\ W_{ij}\\ V_{ij}\\ P_{ij}\end{pmatrix} &= \begin{pmatrix} n_{12}\\ w_{12}\\ v_{12}\\ p_{12}\end{pmatrix}\Theta_i\overline{\Theta}_j,
\end{aligned}
$$

where $n_0, w_0, v_0, p_0, n_{11}, w_{11}, v_{11}, p_{11}, n_{12}, w_{12}, v_{12}, p_{12}$ are known.

For ε^3, we get

$$
\begin{aligned}
L_T\begin{pmatrix} n_3\\ w_3\\ v_3\\ p_3\end{pmatrix} =& \frac{\partial}{\partial T_1}\begin{pmatrix} n_2\\ w_2\\ v_2\\ p_2\end{pmatrix} + \frac{\partial}{\partial T_2}\begin{pmatrix} n_1\\ w_1\\ v_1\\ p_1\end{pmatrix} - \tau_1\begin{pmatrix} m_{11}n_2 + m_{12}w_2 + m_{13}v_2 + m_{14}p_2\\ m_{21}n_2 + m_{22}w_2 + m_{23}v_2 + m_{24}p_2\\ m_{31}n_2 + m_{32}w_2 + m_{33}v_2 + m_{34}p_2\\ m_{41}n_2 + m_{42}w_2 + m_{43}v_2 + m_{44}p_2\end{pmatrix}\\
&- \tau_2 M\begin{pmatrix} m_{11}n_1 + m_{12}w_1 + m_{13}v_1 + m_{14}p_1\\ m_{21}n_1 + m_{22}w_1 + m_{23}v_1 + m_{24}p_1\\ m_{31}n_1 + m_{32}w_1 + m_{33}v_1 + m_{34}p_1\\ m_{41}n_1 + m_{42}w_1 + m_{43}v_1 + m_{44}p_1\end{pmatrix} - \begin{pmatrix} n_1^2 w_1\\ -n_1^2 w_1\\ 0\\ 0\end{pmatrix}\\
=& \begin{pmatrix} E_n\\ E_w\\ E_v\\ E_p\end{pmatrix}.
\end{aligned}
\tag{3.20}
$$

Therefore, the following expression can be derived by the above equation:

$$
\begin{pmatrix} E_n^1\\ E_w^1\\ E_v^1\\ E_p^1\end{pmatrix} = \begin{pmatrix} l_1\frac{\partial P_1}{\partial T_1}\\ l_2\frac{\partial P_1}{\partial T_1}\\ l_3\frac{\partial P_1}{\partial T_1}\\ \frac{\partial P_1}{\partial T_1}\end{pmatrix} + \begin{pmatrix} l_1\frac{\partial \Theta_1}{\partial T_2}\\ l_2\frac{\partial \Theta_1}{\partial T_2}\\ l_3\frac{\partial \Theta_1}{\partial T_2}\\ \frac{\partial \Theta_1}{\partial T_2}\end{pmatrix} - \tau_1\begin{pmatrix} l_1m_{11} + l_2m_{12} + l_3m_{13} + m_{14}\\ l_1m_{21} + l_2m_{22} + l_3m_{23} + m_{24}\\ l_1m_{31} + l_2m_{32} + l_3m_{33} + m_{34}\\ l_1m_{41} + l_2m_{42} + l_3m_{43} + m_{44}\end{pmatrix} P_1
$$

$$
- \tau_2 \begin{pmatrix} l_1 m_{11} + l_2 m_{12} + l_3 m_{13} + m_{14} \\ l_1 m_{21} + l_2 m_{22} + l_3 m_{23} + m_{24} \\ l_1 m_{31} + l_2 m_{32} + l_3 m_{33} + m_{34} \\ l_1 m_{41} + l_2 m_{42} + l_3 m_{43} + m_{44} \end{pmatrix} \Theta_1
+ \begin{pmatrix} G_{11}|\Theta_1|^2 + G_{12}|\Theta_2|^2 + |\Theta_3|^2 \\ G_{21}|\Theta_1|^2 + G_{22}|\Theta_2|^2 + |\Theta_3|^2 \\ 0 \\ 0 \end{pmatrix} \Theta_1, \tag{3.21}
$$

$$
\begin{pmatrix} E_n^2 \\ E_w^2 \\ E_v^2 \\ E_p^2 \end{pmatrix} = \begin{pmatrix} l_1 \frac{\partial P_2}{\partial T_1} \\ l_2 \frac{\partial P_2}{\partial T_1} \\ l_3 \frac{\partial P_2}{\partial T_1} \\ \frac{\partial P_2}{\partial T_1} \end{pmatrix} + \begin{pmatrix} l_1 \frac{\partial \Theta_2}{\partial T_2} \\ l_2 \frac{\partial \Theta_2}{\partial T_2} \\ l_3 \frac{\partial \Theta_2}{\partial T_2} \\ \frac{\partial \Theta_2}{\partial T_2} \end{pmatrix} - \tau_1 \begin{pmatrix} l_1 m_{11} + l_2 m_{12} + l_3 m_{13} + m_{14} \\ l_1 m_{21} + l_2 m_{22} + l_3 m_{23} + m_{24} \\ l_1 m_{31} + l_2 m_{32} + l_3 m_{33} + m_{34} \\ l_1 m_{41} + l_2 m_{42} + l_3 m_{43} + m_{44} \end{pmatrix} P_2 \tag{3.22}
$$

$$
- \tau_2 \begin{pmatrix} l_1 m_{11} + l_2 m_{12} + l_3 m_{13} + m_{14} \\ l_1 m_{21} + l_2 m_{22} + l_3 m_{23} + m_{24} \\ l_1 m_{31} + l_2 m_{32} + l_3 m_{33} + m_{34} \\ l_1 m_{41} + l_2 m_{42} + l_3 m_{43} + m_{44} \end{pmatrix} \Theta_2
+ \begin{pmatrix} G_{11}|\Theta_1|^2 + G_{12}|\Theta_2|^2 + |\Theta_3|^2 \\ G_{21}|\Theta_1|^2 + G_{22}|\Theta_2|^2 + |\Theta_3|^2 \\ 0 \\ 0 \end{pmatrix} \Theta_2,
$$

$$
\begin{pmatrix} E_n^3 \\ E_w^3 \\ E_v^3 \\ E_p^3 \end{pmatrix} = \begin{pmatrix} l_1 \frac{\partial P_3}{\partial T_1} \\ l_2 \frac{\partial P_3}{\partial T_1} \\ l_3 \frac{\partial P_3}{\partial T_1} \\ \frac{\partial P_3}{\partial T_1} \end{pmatrix} + \begin{pmatrix} l_1 \frac{\partial \Theta_3}{\partial T_2} \\ l_2 \frac{\partial \Theta_3}{\partial T_2} \\ l_3 \frac{\partial \Theta_3}{\partial T_2} \\ \frac{\partial \Theta_3}{\partial T_2} \end{pmatrix} - \tau_1 \begin{pmatrix} l_1 m_{11} + l_2 m_{12} + l_3 m_{13} + m_{14} \\ l_1 m_{21} + l_2 m_{22} + l_3 m_{23} + m_{24} \\ l_1 m_{31} + l_2 m_{32} + l_3 m_{33} + m_{34} \\ l_1 m_{41} + l_2 m_{42} + l_3 m_{43} + m_{44} \end{pmatrix} P_3 \tag{3.23}
$$

$$
- \tau_2 \begin{pmatrix} l_1 m_{11} + l_2 m_{12} + l_3 m_{13} + m_{14} \\ l_1 m_{21} + l_2 m_{22} + l_3 m_{23} + m_{24} \\ l_1 m_{31} + l_2 m_{32} + l_3 m_{33} + m_{34} \\ l_1 m_{41} + l_2 m_{42} + l_3 m_{43} + m_{44} \end{pmatrix} \Theta_3
$$

$$+\begin{pmatrix} G_{11}|\Theta_1|^2+G_{12}|\Theta_2|^2+|\Theta_3|^2 \\ G_{21}|\Theta_1|^2+G_{22}|\Theta_2|^2+|\Theta_3|^2 \\ 0 \\ 0 \end{pmatrix}\Theta_3,$$

where $G_{11}=G_{12}=G_{13}=l_1^2l_2, G_{21}=G_{22}=G_{23}=-l_1^2l_2$.

By the Fredholm solvability condition, then it is combined with (3.21)-(3.23) allows us to deduce the following expression:

$$\begin{cases} (l_1+l_2l_2^++l_3l_3^++l_4^+)(\frac{\partial P_1}{\partial T_1}+\frac{\partial \Theta_1}{\partial T_2}) \\ =(\tau_1P_1+\tau_2\Theta_1)[(l_1m_{11}+l_2m_{12}+l_3m_{13}+m_{14})+l_2^+(l_1m_{21}+l_2m_{22}+l_3m_{23} \\ \quad +m_{24})+l_3^+(l_1m_{31}+l_2m_{32}+l_3m_{33}+m_{34})+l_4^+(l_1m_{41}+l_2m_{42}+l_3m_{43} \\ \quad +m_{44})]-(G_{11}|\Theta_1|^2+G_{12}|\Theta_2|^2+|\Theta_3|^2)\Theta_1-l_2^+(-G_{11}|\Theta_1|^2-G_{12}|\Theta_2|^2 \\ \quad +|\Theta_3|^2)\Theta_1, \\ (l_1+l_2l_2^++l_3l_3^++l_4^+)(\frac{\partial P_2}{\partial T_1}+\frac{\partial \Theta_2}{\partial T_2}) \\ =(\tau_1P_2+\tau_2\Theta_2)[(l_1m_{11}+l_2m_{12}+l_3m_{13}+m_{14})+l_2^+(l_1m_{21}+l_2m_{22}+l_3m_{23} \\ \quad +m_{24})+l_3^+(l_1m_{31}+l_2m_{32}+l_3m_{33}+m_{34})+l_4^+(l_1m_{41}+l_2m_{42}+l_3m_{43} \\ \quad +m_{44})]-(G_{11}|\Theta_1|^2+G_{12}|\Theta_2|^2+|\Theta_3|^2)\Theta_2-l_2^+(-G_{11}|\Theta_1|^2-G_{12}|\Theta_2|^2 \\ \quad +|\Theta_3|^2)\Theta_2, \\ (l_1+l_2l_2^++l_3l_3^++l_4^+)(\frac{\partial P_3}{\partial T_1}+\frac{\partial \Theta_3}{\partial T_2}) \\ =(\tau_1P_3+\tau_2W_3)[(l_1m_{11}+l_2m_{12}+l_3m_{13}+m_{14})+l_2^+(l_1m_{21}+l_2m_{22}+l_3m_{23} \\ \quad +m_{24})+l_3^+(l_1m_{31}+l_2m_{32}+l_3m_{33}+m_{34})+l_4^+(l_1m_{41}+l_2m_{42}+l_3m_{43} \\ \quad +m_{44})]-(G_{11}|\Theta_1|^2+G_{12}|\Theta_2|^2+|\Theta_3|^2)\Theta_3-l_2^+(-G_{11}|\Theta_1|^2-G_{12}|\Theta_2|^2 \\ \quad +|\Theta_3|^2)\Theta_3. \end{cases} \tag{3.24}$$

Let $A_i=A_i^n=l_3A_i^w=l_2A_i^v=l_1A_i^p$ be the coefficient of $e^{i\vec{k_j}\cdot\vec{r}}$ $(j=1,2,3)$, then

$$\begin{pmatrix} A_i^n \\ A_i^w \\ A_i^v \\ A_i^p \end{pmatrix} = \varepsilon \begin{pmatrix} l_1 \\ l_2 \\ l_3 \\ 1 \end{pmatrix} W_i + \varepsilon^2 \begin{pmatrix} l_1 \\ l_2 \\ l_3 \\ 1 \end{pmatrix} P_i + o(\varepsilon^3), i=1,2,3. \tag{3.25}$$

Multiply (3.18) by ε and multiply (3.24) by ε^2, and merge variables using (3.8) and (3.25). Therefore, the following equation is obtained:

$$\begin{cases} \epsilon_0\frac{\partial A_1}{\partial t}=\xi A_1+h\overline{A}_2\overline{A}_3-[\alpha_1|A_1|^2+\alpha_2(|A_2|^2+|A_3|^2)]A_1, \\ \epsilon_0\frac{\partial A_2}{\partial t}=\xi A_2+h\overline{A}_1\overline{A}_3-[\alpha_1|A_2|^2+\alpha_2(|A_1|^2+|A_3|^2)]A_2, \\ \epsilon_0\frac{\partial A_3}{\partial t}=\xi A_3+h\overline{A}_1\overline{A}_2-[\alpha_1|A_3|^2+\alpha_2(|A_1|^2+|A_2|^2)]A_3, \end{cases} \tag{3.26}$$

where,

$$\begin{aligned}
&\epsilon_0 = -\frac{l_1 + l_2 l_2^+ + l_3 l_3^+ + l_4^+}{q\tau_T},\ \xi = -\frac{\tau_T - \tau}{\tau_T},\ h = \frac{l_2 l_3}{q\tau_T},\\
&\alpha_1 = -\frac{G_{11} + l_2^+ G_{21}}{q\tau_T},\ \alpha_2 = -\frac{G_{21} + l_2^+ G_{22}}{q\tau_T},\\
&q = (l_1 m_{11} + l_2 m_{12} + l_3 m_{13} + m_{14}) + l_2^+(l_1 m_{21} + l_2 m_{22} + l_3 m_{23} + m_{24})\\
&\quad + l_3^+(l_1 m_{31} + l_2 m_{32} + l_3 m_{33} + m_{34}) + l_4^+(l_1 m_{41} + l_2 m_{42} + l_3 m_{43} + m_{44}).
\end{aligned}$$

Substituting $A_i = \vartheta_i e^{i\varsigma_i}$ into (3.26), we can obtain the following form:

$$\begin{cases}
\epsilon_0 \frac{\partial \varsigma}{\partial t} = -h\frac{\vartheta_1^2\vartheta_2^2 + \vartheta_1^2\vartheta_3^2 + \vartheta_2^2\vartheta_3^2}{\vartheta_1\vartheta_2\vartheta_3},\\
\epsilon_0 \frac{\partial \vartheta_1}{\partial t} = \sigma\vartheta_1 + h\vartheta_2\vartheta_3 cos\varsigma - \alpha_1\vartheta_1^3 - \alpha_2(\vartheta_2^2 + \vartheta_3^2)\vartheta_1,\\
\epsilon_0 \frac{\partial \vartheta_2}{\partial t} = \sigma\vartheta_2 + h\vartheta_1\vartheta_3 cos\varsigma - \alpha_1\vartheta_2^3 - \alpha_2(\vartheta_1^2 + \vartheta_3^2)\vartheta_2,\\
\epsilon_0 \frac{\partial \vartheta_3}{\partial t} = \sigma\vartheta_3 + h\vartheta_1\vartheta_2 cos\varsigma - \alpha_1\vartheta_3^3 - \alpha_2(\vartheta_1^2 + \vartheta_2^2)\vartheta_3,
\end{cases} \tag{3.27}$$

where $\varsigma = \varsigma_1 + \varsigma_2 + \varsigma_3$.

System (3.27) corresponds to four kinds of different pattern structures. Table 1 shows that the corresponding generation conditions of four different pattern structures.

Table 1. Four different pattern structures corresponding to the generation conditions

Pattern structure	Expression	Generation conditions
mixed state	$\vartheta_1 = \frac{\lvert h\rvert}{\alpha_2 - \alpha_1}, \vartheta_2 = \vartheta_3 = \sqrt{\frac{\sigma - \alpha_1\vartheta_1^2}{\alpha_2 + \alpha_1}}$	$\alpha_2 > \alpha_1, \sigma > \sigma_3 = \frac{h^2\alpha_1}{(\alpha_2 - \alpha_1)^2}$
spots pattern	$\vartheta_1 = \vartheta_2 = \vartheta_3 = \frac{\lvert h\rvert \pm\sqrt{h^2 + 4(\alpha_1 + 2\bar{g}_2)\sigma}}{2(\alpha_1 + 2\alpha_2)}$	$\sigma > \sigma_1 = \frac{-h^2}{4(\alpha_1 + 2\alpha_2)}$
stripes pattern	$\vartheta_1 = \sqrt{\frac{\sigma}{\alpha_1}}, \vartheta_2 = \vartheta_3 = 0$	$\sigma > 0$
stationary state	$\vartheta_1 = \vartheta_2 = \vartheta_3 = 0$	always

4. Numerical results

We conduct numerical simulations according to the results of the above theoretical analysis in this part. The boundary condition is the Neumann boundary condition. The space region studied is a two-dimensional space region with a size of $[0, 100] \times [0, 100]$, the time interval is 500. The space and time steps are $\Delta x = 1$ and $\Delta t = 0.001$, respectively. Several types of vegetation patterns are obtained by using multi-scale theory. The following is mainly to study the effect of intensity of nonlocal effect τ and diffusion coefficient β on vegetation pattern.

Selecting the following parameter values: $\eta = 2.6, \gamma = 1.2$. Through calculation, the parameters values can be obtained: $h = \frac{l_2 l_3}{q\tau_T}, \alpha_1 = -\frac{G_{11} + l_2^+ G_{21}}{q\tau_T}, \alpha_2 = -\frac{G_{21} + l_2^+ G_{22}}{q\tau_T}, \sigma_1 = \frac{-h^2}{4(\alpha_1 + 2\alpha_2)}, \sigma_2 = 0, \sigma_3 = \frac{h^2\alpha_1}{(\alpha_2 - \alpha_1)^2}, \sigma_4 = \frac{(2\alpha_1 + \alpha_2)h^2}{(\alpha_2 - \alpha_1)^2}$ can be given. According to reference [21], the pattern structure corresponding to different control parameters is shown in Table 2.

We choose $\tau = 0.22$ and other parameters can be obtained $h = \frac{l_2 l_3}{q\tau_T}, \sigma = 0.6273504, \sigma_3 = 4.3764255$. Obviously, inequality $0 = \sigma_2 < \sigma < \sigma_3$ holds and

Table 2. The pattern structure corresponding to different control parameters

Interval	Pattern structure
$\sigma \in (\sigma_2, \sigma_3)$	spot pattern
$\sigma \in (\sigma_3, \sigma_4)$	mixed pattern
$\sigma \in (\sigma_4, +\infty)$	stripe pattern

system (2.7) will present spot pattern. Fig. 3 shows that the temporal succession of vegetation pattern when $\tau = 0.22, \beta = 30$. The vegetation is uniformly distributed at the start. With the increase of time, the vegetation pattern becomes spot pattern, and the vegetation gathers together in the form of clusters. Fig. 4 shows that the evolution of water pattern over time. By comparing Fig. 3 and Fig. 4, it can be concluded that the densities of vegetation and water present a reverse relationship at the same location which is related to the local soil quality [37].

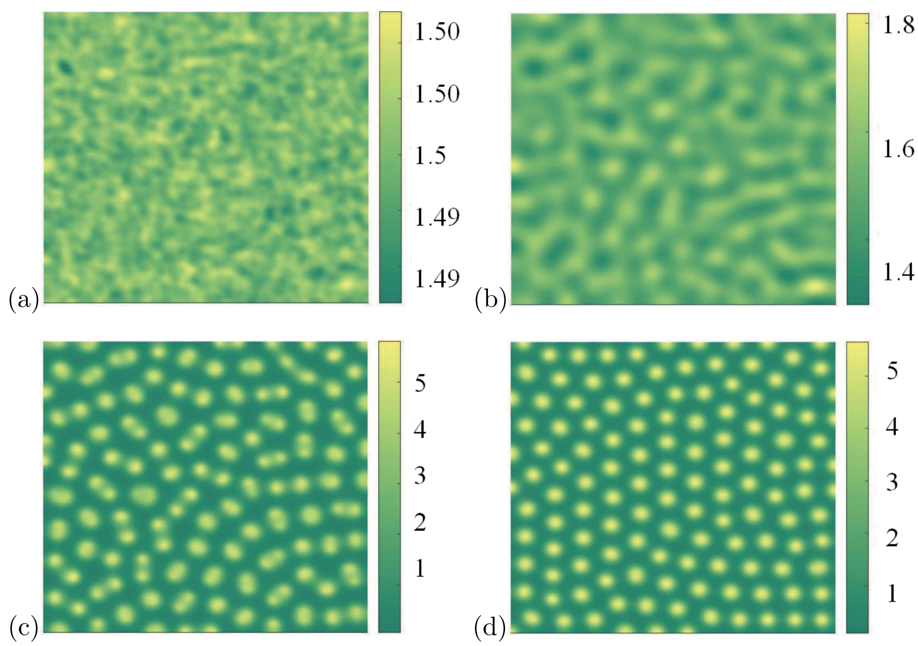

Figure 3. When $\tau = 0.22$, the evolution of vegetation pattern over time. The pattern finally presents spot structure. Other parameters are fixed as: $\eta = 2.6, \gamma = 1.2, \beta = 30$. The evolution process of pattern is $(a) \to (b) \to (c) \to (d)$.

In order to explore the influences of diffusion coefficient β on vegetation pattern, the simulation results are shown in Figure 5. Obviously, the pattern structure changes with increase of β. When $\beta = 8$, vegetation pattern shows the stripe structure and control parameter σ is greater σ_4 (Fig. 5(a)). With the increase of β, strip pattern loses stability and spot pattern appears gradually, now σ is between σ_3 and σ_4, and the mixed patterns appear in Fig. 5(b). When β increases further, pattern shows spot structure in Fig. 5(c) and Fig. 5(d), and σ is between σ_2 and σ_3. In the process, the stripe pattern disappears gradually and the whole space presents spot pattern structure [21]. One can conclude that with the increase of diffusion coefficient, the change of pattern structure is as follows: stripe pattern$\longrightarrow$mixed

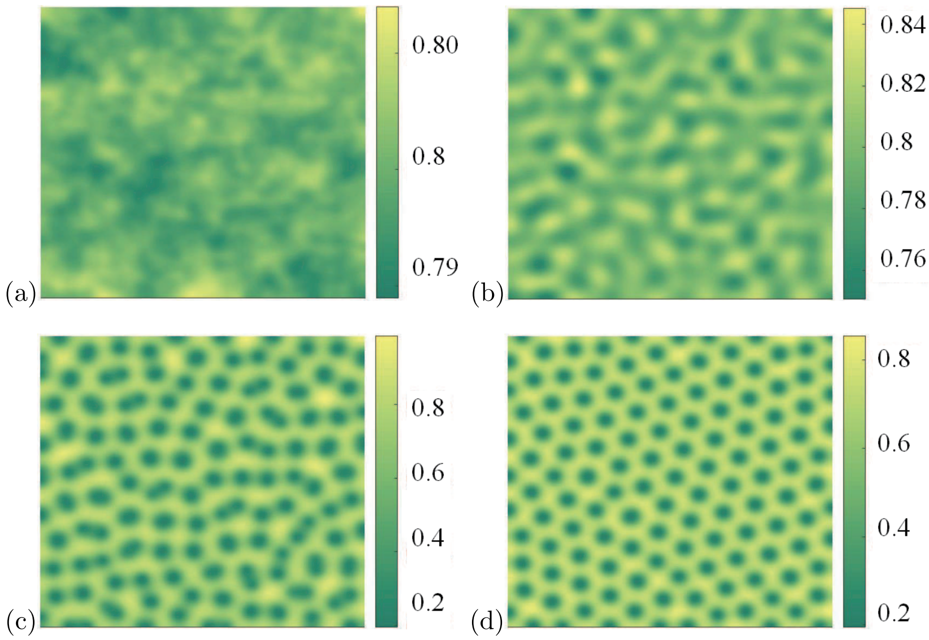

Figure 4. When $\tau = 0.22$, the evolution of water density over time. Other parameters are fixed as: $\eta = 2.6, \gamma = 1.2, \beta = 30$. The evolution process of pattern is $(a) \rightarrow (b) \rightarrow (c) \rightarrow (d)$.

pattern$\longrightarrow$ spot pattern.

Moreover, we run another set of simulations for different τ in Fig. 6 with $\eta = 2.6, \gamma = 1.2, \beta = 30$. As can be seen from Fig. 6, the number of spot patterns increases with the increase of τ. This means the number of vegetation clusters formed increases. Besides, that vegetation forms smaller clusters as the intensity of nonlocal effect increases by numerical simulation. One can conclude that the isolation degree of vegetation pattern increases which is not conducive to the robustness of the ecosystem.The spatial distribution of vegetation is shown in Fig. 7 which is more intuitively.

In order to further study the influence of parameter values on pattern formation, we carry out relevant numerical simulation. In Fig. 8, we plot the effect τ on the recovery rate and recovery time. Select the initial state of steady-state pattern at $\tau = 0.24$, the time required for different τ to reach the initial state under small perturbation is simulated which is called recovery time. The recovery rate is the rate at which the initial state is reached and is as shown in Figure 8(b). The results show that the recovery time decrease gradually with the increase of τ. On the contrary, the recovery rate increases as τ increases, that is, τ is more closer to 2.4 and the recovery rate is more higher.

5. Conclusions and discussions

In this study, the nonlocal delay term with strong kernel is introduced into the vegetation-water model which is considered the nonlocal effect of water uptake by vegetation roots. A two-variable model with nonlocal delay is transformed into a four-variable reaction diffusion equation. Through mathematical analysis, we

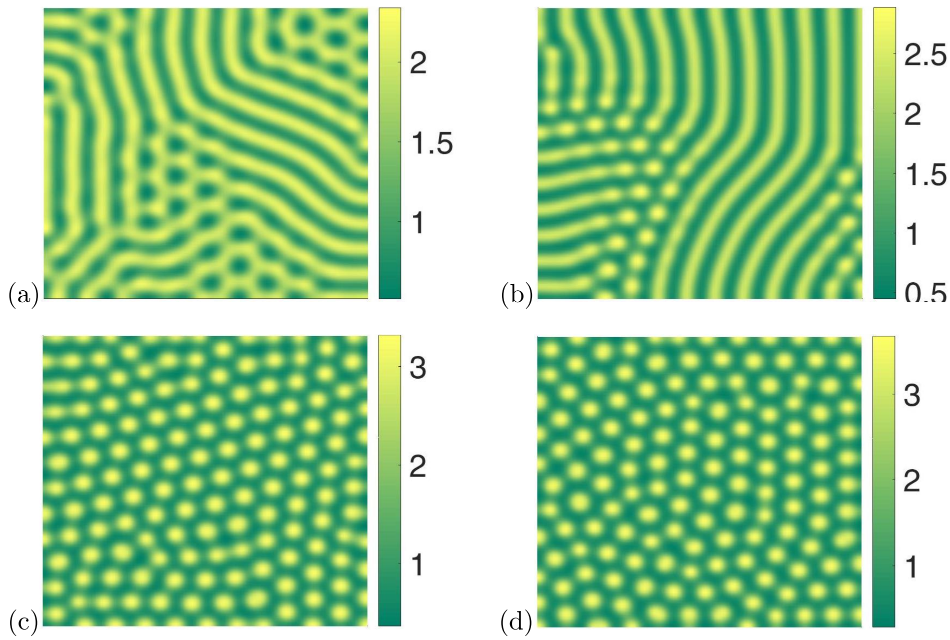

Figure 5. Different β corresponds to the vegetation patterns. With the increase of β, the pattern changes from stripe structure to spot structure. Other parameters are fixed as: $\eta = 2.6, \gamma = 1.2, \tau = 0.22$. (a) $\beta = 8$; (b) $\beta = 10$; (c) $\beta = 12$; (d) $\beta = 14$.

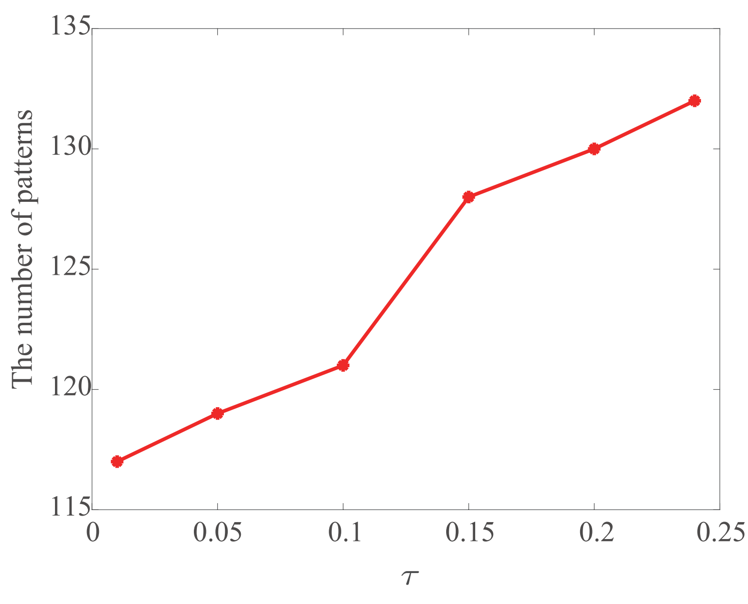

Figure 6. The number of spot patterns at different parameter τ with $\eta = 2.6, \gamma = 1.2, \beta = 30$.

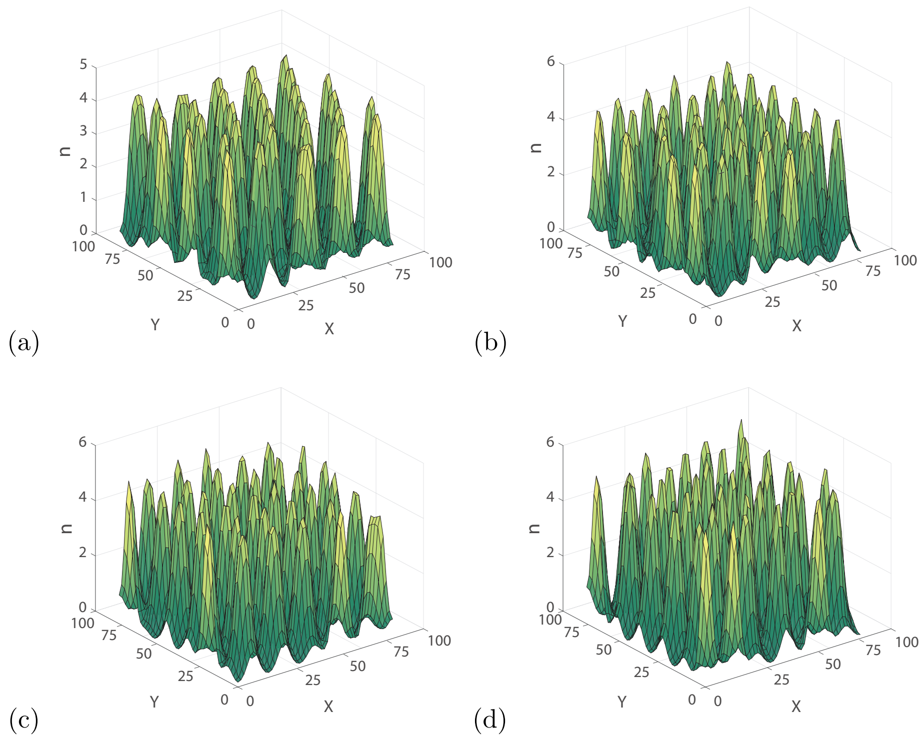

Figure 7. Different τ corresponds to the spatial distribution of vegetation. Other parameters are fixed as: $\eta = 2.6, \gamma = 1.2, \beta = 30$. (a) $\tau = 0.01$; (b) $\tau = 0.1$; (c) $\tau = 0.15$; (d) $\tau = 0.24$.

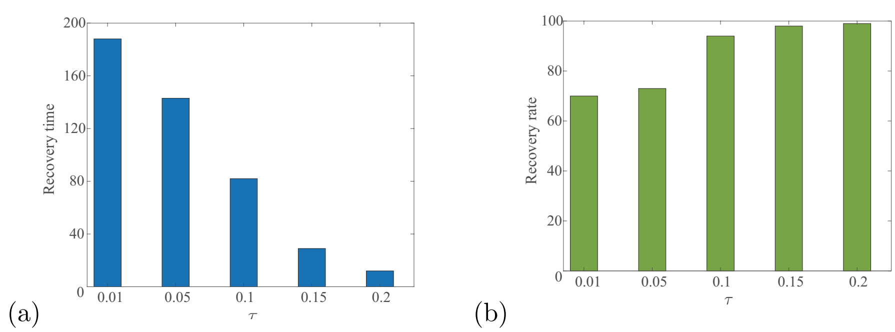

Figure 8. Different τ corresponds to recovery time and recovery rate. Other parameters are fixed as: $\eta = 2.6, \gamma = 1.2, \beta = 30$. (a) Recovery time; (b) Recovery rate. The recovery time is negatively correlated with τ and the recovery rate is positively correlated with τ.

deduce the conditions for stability of ODE model and Turing instability of the model with diffusion. The amplitude equation is derived from the theory of multi-scale analysis. According to the coefficients of the amplitude equation, the four kinds of structures and stability of the pattern can be determined.

By numerical simulations, the relation between intensity of nonlocal effect τ and vegetation density is obtained. The results show that the isolation degree of vegetation pattern increases as τ increases, the increased intensity of nonlocal effect is not conducive to improving the robustness of the ecosystem which provides a theoretical basis for vegetation protection. Our results point to the recovery time is negatively correlated with τ, and the recovery rate is positively correlated with τ which implies that the effect of τ on ecosystem resilience.

We next explore the effect of diffusion coefficient of water on pattern structure. The results show that the increase of β leads to the change of pattern structure: stripe pattern→mixed pattern→spot pattern. This implies that water diffusion has an important influence on vegetation distribution and may lead to desertification in this area.

It is worth noting that strong kernel are studied in this paper, which is very different from the weak kernel. In fact, the roots of vegetation not only absorb water at the current location, but also absorb water near the roots over a certain period of time, which suggests that it is necessary to introduce nonlocal effect into the vegetation model. We expand on the existing work and specifically study the effect of strong kernel on vegetation distribution. According to the numerical simulations of strong kernel, we can get that the intensity of water absorption by roots of vegetation increases firstly and then decreases which is more consistent with the characteristics of water absorption by vegetation in arid and semi-arid regions. It can be seen from our conclusions that the nonlocal delay plays a great role in vegetation growth. Our findings provide a theoretical basis for vegetation protection and early warning of desertification.

It is rewarding mentioning that our methods and results can also be applied to other fields, such as infectious disease models [2, 33, 47], population models [64, 69] and so on. Meanwhile, the slope is also a significant factor for vegetation growth. Hence, the vegetation system should be coupled with the slope factor. An interesting topic for future work is that the noise factors and meteorological factors (e.g., temperature, light and rainfall) are coupled into the vegetation model and the future vegetation distribution is predicted based on the actual data [49, 51, 56].

Acknowledgements

National Natural Science Foundation of China under Grant nos. 42075029 and 42275034, Outstanding Young Talents Support Plan of Shanxi province, Fundamental Research Program of Shanxi Province (Grant nos. 202203021212327, 202203021211213), Program for the (Reserved) Discipline Leaders of Taiyuan Institute of Technology.

Data availability statement

Data sharing not applicable to this article as no datasets were generated or analysed during the current study.

Declaration of interests

The authors report no conflicts of interest. The authors alone are responsible for the content and writing of this article.

References

[1] M. Alfaro, J. Coville and G. Raoul, *Travelling waves in a nonlocal reaction-diffusion equation as a model for a population structured by a space variable and a phenotypic trait*, Commun. Part. Diff. Eq., 2013, 38(12), 2126–2154.

[2] N. Bai and R. Xu, *Mathematical analysis of an HIV model with latent reservoir, delayed ctl immune response and immune impairment*, Math. Biosci. Eng., 2021, 18(2), 1689–1707.

[3] J. A. Bonachela, R. M. Pringle, E. Sheffer, et al., *Termite mounds can increase the robustness of dryland ecosystems to climatic change*, Science, 2015, 347(6222), 651–655.

[4] F. Borgogno, P. Dodorico, F. Laio and L. Ridolfi, *Mathmatical models of vegetation pattern formation in ecohydrology*, Rev. Geophysics, 2009, 47(1), RG1005.

[5] K. Boushaba and S. G. Ruan, *Instability in diffusive ecological models with nonlocal delay effects*, J. Math. Anal. Appl., 2001, 258, 269–286.

[6] S. Chen and J. Shi, *Stability and Hopf bifurcation in a diffusive logistic population model with nonlocal delay effect*, J. Differ. Equations, 2012, 253(12), 3440–3470.

[7] C. Dineshkumar, R. Udhayakumar, V. Vijayakumar, et al., *A note on approximate controllability for nonlocal fractional evolution stochastic integrodifferential inclusions of order $r \in (1, 2)$ with delay*, Chaos Soliton. Fract., 2021, 153, 111565.

[8] A. Doelman and H. van der Ploeg, *Homoclinic stripe patterns*, SIAM J. Appl. Dyn. Syst., 2002, 1(1), 65–104.

[9] L. Eigentler and J. A. Sherratt, *Analysis of a model for banded vegetation patterns in semi-arid environments with nonlocal dispersal*, J. Math. Biol., 2018, 77, 739–763.

[10] M. Fuentes, M. Kuperman and V. Kenkre, *Nonlocal interaction effects on pattern formation in population dynamics*, Theor. Popul. Biol., 2003, 91(15), 158104.

[11] S. Getzin, H. Yizhaq, B. Belld, et al., *Discovery of fairy circles in Australia supports self-organization theory*, P. Natl. Acad. Sci. USA, 2016, 113(13), 3551–3556.

[12] E. Gilad, J. von Hardenberg, A. Provenzale, et al., *A mathematical model of plants as ecosystem engineers*, J. Theor. Biol., 2007, 244(4), 680–691.

[13] S. Gourley, M. A. Chaplain and F. Davidson, *Spatio-temporal pattern formation in a nonlocal reaction-diffusion equation*, Dynam. Syst., 2001, 16(2), 173–192.

[14] S. A. Gourley and S. Ruan, *Spatio-temporal delays in a nutrient-plankton model on a finite domain: Linear stability and bifurcations*, Appl. Math. Comput., 2003, 145(2–3), 391–412.

[15] S. A. Gourley and J. W. H. So, *Dynamics of a food-limited population model incorporating nonlocal delays on a finite domain*, J. Math. Biol., 2002, 44, 49–78.

[16] K. Gowda, H. Riecke and M. Silber, *Transitions between patterned states in vegetation models for semiarid ecosystems*, Phys. Rev. E, 2014, 89(2), 022701.

[17] S. J. Guo, *Stability and bifurcation in a reaction-diffusion model with nonlocal delay effect*, J. Differ. Equations, 2015, 259(4), 1409–1448.

[18] S. J. Guo and S. L. Yan, *Hopf bifurcation in a diffusive Lotka-Volterra type system with nonlocal delay effect*, J. Differ. Equations, 2016, 260(1), 781–817.

[19] S. J. Guo and J. Zimmer, *Stability of travelling wavefronts in discrete reaction-diffusion equations with nonlocal delay effects*, Nonlinearity, 2015, 28(2), 463–492.

[20] Z. G. Guo, G. Q. Sun, Z. Wang, et al., *Spatial dynamics of an epidemic model with nonlocal infection*, Appl. Math. Comput., 2020, 377, 125158.

[21] B. S. Han and Z. C. Wang, *Turing patterns of a Lotka-Volterra competitive system with nonlocal delay*, Int. J. Bifurcat. Chaos, 2018, 28(7), 1830021.

[22] R. HilleRisLambers, M. Rietkerk, F. van den Bosch, et al., *Vegetation pattern formation in semi-arid grazing systems*, Ecology, 2001, 82(1), 50–61.

[23] L. F. Hou, S. P. Gao and G. Q. Sun, *Two types of fairy circles coexist in a vegetation-water model*, Nonlinear Dynam., 2023, 111(8), 7883–7898.

[24] L. F. Hou, G. Q. Sun and M. Perc, *The impact of heterogeneous human activity on vegetation patterns in arid environments*, Commun. Nonlinear Sci., 2023, 126, 107461.

[25] B. J. Kealy and D. J. Wollkind, *A nonlinear stability analysis of vegetative turing pattern formation for an interaction-diffusion plant-surface water model system in an arid flat environment*, B. Math. Biol., 2012, 74(4), 803–833.

[26] S. Kéfi, M. Rietkerk, C. L. Alados, et al., *Spatial vegetation patterns and imminent desertification in mediterranean arid ecosystems*, Nature, 2007, 449(7159), 213–217.

[27] S. Kéfi, M. Rietkerk and G. G. Katul, *Vegetation pattern shift as a result of rising atmospheric CO_2 in arid ecosystems*, Theor. Popul. Biol., 2008, 74(4), 332–344.

[28] S. Kéfi, M. Rietkerk, M. van Baalen and M. Loreau, *Local facilitation, bistability and transitions in arid ecosystems*, Theor. Popul. Biol., 2007, 71, 367–379.

[29] C. A. Klausmeier, *Regular and irregular patterns in semiarid vegetation*, Science, 1999, 284, 1826–1828.

[30] A. Kletter, J. von Hardenberg, E. Meron and A. Provenzale, *Patterned vegetation and rainfall intermittency*, J. Theor. Biol., 2009, 256(4), 574–583.

[31] R. Lefever and O. Lejeune, *On the origin of tiger bush*, B. Math. Biol., 1997, 59, 263–294.

[32] O. Lejeune, M. Tildi and R. Lefever, *Vegetation spots and stripes: Dissipative structures in arid landscapes*, Int. J. Quantum Chem., 2004, 98(2), 261–271.

[33] H. J. Li, W. Xu, S. Song, et al., *The dynamics of epidemic spreading on signed networks*, Chaos Soliton. Fract., 2021, 151, 111294.

[34] J. Li, G. Q. Sun and Z. G. Guo, *Bifurcation analysis of an extended Klausmeier-Gray-Scott model with infiltration delay*, Stud. Appl. Math., 2022, 148, 1519–1542.

[35] J. Li, G. Q. Sun and Z. Jin, *Interactions of time delay and spatial diffusion induce the periodic oscillation of the vegetation system*, Discre. Cont. Dyn.-B, 2022, 27, 2147–2172.

[36] W. T. Li, G. Lin, C. Ma and F. Y. Yang, *Traveling wave solutions of a nonlocal delayed SIR model without outbreak threshold*, Discre. Cont. Dyn.-B, 2014, 19(2), 467–484.

[37] J. Liang, C. liu, G. Q. Sun, et al., *Nonlocal interactions between vegetation induce spatial patterning*, Appl. Math. Comput., 2022, 428, 127061.

[38] G. Lin and W. T. Li, *Bistable wavefronts in a diffusive and competitive Lotka-Volterra type system with nonlocal delays*, J. Differ. Equations, 2008, 244(3), 487–513.

[39] G. Lin and S. G. Ruan, *Traveling wave solutions for delayed reaction-diffusion systems and applications to diffusive Lotka-Volterra competition models with distributed delays*, J. Dyn. Differ. Equ., 2014, 26(3), 583–605.

[40] G. Y. Lv and M. X. Wang, *Traveling wave front and stability as planar wave of reaction diffusion equations with nonlocal delays*, Z. Angew. Math. Phys., 2013, 64(4), 1005–1023.

[41] R. M. May, *Thresholds and breakpoints in ecosystems with a multiplicity of stable states*, Nature, 1977, 269, 471–477.

[42] S. M. Merchant and W. Nagata, *Instabilities and spatiotemporal patterns behind predator invasions with nonlocal prey competition*, Theor. Popul. Biol., 2011, 80(4), 289–297.

[43] F. I. Pugnaire and M. T. Luque, *Changes in plant interactions along a gradient of environmental stress*, Oikos, 2001, 93(1), 42–49.

[44] J. A. Sherratt, *An analysis of vegetation stripe formation in semi-arid landscapes*, J. Math. Biol., 2005, 51, 183–197.

[45] J. P. Shi, Z. F. Xie and K. Little, *Cross-diddusion induce instability and stability in reaction-diffusion system*, J. Appl. Anal. Comput., 2011, 1(1), 95–119.

[46] E. Siero, A. Doelman, M. B. Eppinga, et al., *Striped pattern selection by advective reaction-diffusion systems: Resilience of banded vegetation on slopes*, Chaos, 2015, 25(3), 036411.

[47] H. T. Song, G. H. Fan, S. Zhao, et al., *Forecast of the COVID–19 trend in India: A simple modelling approach*, Math. Biosci. Eng., 2021, 18(6), 9775–9786.

[48] Y. L. Song, S. H. Wu and H. Wang, *Spatiotemporal dynamics in the single population model with memory-based diffusion and nonlocal effect*, J. Differ. Equations, 2019, 267(11), 6316–6351.

[49] M. J. Steinbauer, J. A. Grytnes, G. Jurasinski, et al., *Accelerated increase in plant species richness on mountain summits is linked to warming*, Nature, 2018, 556, 231–250.

[50] G. Q. Sun, M. Jusup, Z. Jin, et al., *Pattern transitions in spatial epidemics: Mechanisms and emergent properties*, Phys. Life Rev., 2016, 19, 43–73.

[51] G. Q. Sun, L. Li, J. Li, et al., *Impacts of climate change on vegetation pattern: Mathematical modelling and data analysis*, Phys. Life Rev., 2022, 43, 239–270.

[52] G. Q. Sun, C. H. Wang, L. L. Chang, et al., *Effects of feedback regulation on vegetation patterns in semi-arid environments*, Appl. Math. Model., 2018, 61, 200–215.

[53] G. Q. Sun, H. T. Zhang, Y. L. Song, et al., *Dynamic analysis of a plant-water model with spatial diffusion*, J. Differ. Equations, 2022, 329, 395–430.

[54] Q. L. Tang, J. Ge and Z. G. Lin, *An SEI-SI avian-human influenza model with diffusion and nonlocal delay*, Appl. Math. Comput., 2014, 247, 753–761.

[55] S. Thompson, G. Katul, J. Terborgh and P. Alvarez-Loayza, *Spatial organization of vegetation arising from non-local excitation with local inhibition in tropical rainforests*, Physica D, 2009, 238, 1061–1067.

[56] C. J. Tucker, I. Y. Fungt, C. D. Keeling and R. H. Gammon, *Relationship between atmospheric CO_2 variations and a satellite-derived vegetation index*, Nature, 1986, 319, 195–198.

[57] J. von Hardenberg, E. Meron, M. Shachak and Y. Zarmi, *Diversity of vegetation patterns and desertification*, Phys. Rev. Lett., 2001, 87(19), 198101.

[58] J. van de Koppel, M. Rietkerk and F. J. Weissing, *Catastrophic vegetation shifts and soil degradation in terrestrial grazing systems*, Trends Ecol. Evol., 1997, 12, 352–356.

[59] J. B. Wang, W. T. Li and F. Y. Yang, *Traveling waves in a nonlocal dispersal SIR model with nonlocal delayed transmission*, Commun. Nonlinear Sci., 2015, 27(1–3), 136–152.

[60] M. X. Wang and G. Lv, *Entire solutions of a diffusive and competitive Lotka-Volterra type system with nonlocal delays*, Nonlinearity, 2010, 23(7), 1609–1630.

[61] Z. C. Wang, W. T. Li and S. G. Ruan, *Existence and stability of traveling wave fronts in reaction advection diffusion equations with nonlocal delay*, J. Differ. Equations, 2007, 238(1), 153–200.

[62] Z. C. Wang, W. T. Li and S. G. Ruan, *Traveling fronts in monostable equations with nonlocal delayed effects*, J. Dyn. Differ. Equ., 2008, 20(3), 573–607.

[63] Z. C. Wang, W. T. Li and S. G. Ruan, *Entire solutions in bistable reaction-diffusion equations with nonlocal delayed nonlinearity*, Tra. Amer. Soc., 2009, 361(4), 2047–2084.

[64] S. Wu, J. Shi and B. Wu, *Global existence of solutions and uniform persistence of a diffusive predator-prey model with prey-taxis*, J. Differ. Equations, 2016, 26(7), 5847–5874.

[65] R. Xu, M. A. J. Chaplain and F. A. Davidson, *Travelling wave and covetgence in stage-structured reaction-diffusion competitive models with nonlocal delays*, Chaos Soliton. Fract., 2006, 30, 974–992.

[66] Q. Xue, C. Liu, L. Li, et al., *Interactions of diffusion and nonlocal delay give rise to vegetation patterns in semi-arid environments*, Appl. Math. Comput., 2021, 399, 126038.

[67] S. Zaytseva, J. P. Shi and L. B Shaw, *Model of pattern formation in marsh ecosystems with nonlocal interactions*, J. Math. Biol., 2019, 86, 655–686.

[68] L. Zhang and Z. G. Lin, *A Höllings type II prey-predator model with stage structure and nonlocal delay*, Appl. Math. Comput., 2011, 217(10), 5000–5010.

[69] J. D. Zhao and T. H. Zhang, *Dynamics of two predator-prey models with power law pelation*, J. Appl. Anal. Comput., 2023, 13(1), 233–248.